



**Kaunas University of Technology**  
Faculty of Mechanical Engineering and Design

# **Investigation of Robotic Incremental Formation of Polymer Sheet**

Master's Final Degree Project

---

**Baltramiejus Andrijaitis**

Project author

**Lect. Darius Eidukynas**

Supervisor

---

**Kaunas, 2022**



**Kaunas University of Technology**  
Faculty of Mechanical Engineering and Design

# **Investigation of Robotic Incremental Formation of Polymer Sheet**

Master's Final Degree Project  
Mechatronics (6211EX017)

---

**Baltramiejus Andrijaitis**

Project author

**Lect. Darius Eidukynas**

Supervisor

**Prof. Vytautas Jūrėnas**

Reviewer

---

**Kaunas, 2022**



**Kaunas University of Technology**

Faculty of Mechanical Engineering and Design

Baltramiejus Andrijaitis

# **Investigation of Robotic Incremental Formation of Polymer Sheet**

## **Declaration of Academic Integrity**

I confirm the following:

1. I have prepared the final degree project independently and honestly without any violations of the copyrights or other rights of others, following the provisions of the Law on Copyrights and Related Rights of the Republic of Lithuania, the Regulations on the Management and Transfer of Intellectual Property of Kaunas University of Technology (hereinafter – University) and the ethical requirements stipulated by the Code of Academic Ethics of the University;
2. All the data and research results provided in the final degree project are correct and obtained legally; none of the parts of this project are plagiarized from any printed or electronic sources; all the quotations and references provided in the text of the final degree project are indicated in the list of references;
3. I have not paid anyone any monetary funds for the final degree project or the parts thereof unless required by the law;
4. I understand that in the case of any discovery of the fact of dishonesty or violation of any rights of others, the academic penalties will be imposed on me under the procedure applied at the University; I will be expelled from the University and my final degree project can be submitted to the Office of the Ombudsperson for Academic Ethics and Procedures in the examination of a possible violation of academic ethics.

Baltramiejus Andrijaitis

*Confirmed electronically*



**Kaunas University of Technology**

Faculty of Mechanical Engineering and Design

**Task of the Master's final degree project**

**Given to the student** – Baltramiejus Andrijaitis

**1. Title of the project**

Investigation of Robotic Incremental Formation of Polymer Sheet

*(In English)*

Polimero lakšto robotizuoto palaipsninio formavimo tyrimas

*(In Lithuanian)*

**2. Hypothesis:**

Single point tool heating in robotic incremental forming of polymer sheet improves the quality of the sheet and reduces energy consumption.

**3. Aim and tasks of the project**

Aim: To investigate the incremental forming of polymer sheets using a single-point heating tool.

Tasks:

1. To design a self-heating forming tool for incremental single point forming.
2. To conduct experimental research on the designed self-heated tool.
3. To make a simulation of heated tool incremental forming forces on polymer sheet.
4. To perform robotic incremental forming of polymer sheet using developed single point heating tool.

**4. Initial data of the project**

To form round samples achieving at least 20 mm forming depth of 2 mm thickness sheets. Feed rate at least 50 mm/s. Maximum heating time 500 s.

**5. Main requirements and conditions**

SolidWorks, ANSYS, polymer PVC Trovidur ESA-D, ABB IRB1200 manipulator.

Project author	Baltramiejus Andrijaitis	2022.02.28
	<i>(Name, Surname)</i>	<i>(Date)</i>
	<i>(Signature)</i>	
Supervisor	Darius Eidukynas	2022.02.28
	<i>(Name, Surname)</i>	<i>(Date)</i>
	<i>(Signature)</i>	
Head of study field programs	Regita Bendikienė	2022.02.28
	<i>(Name, Surname)</i>	<i>(Date)</i>
	<i>(Signature)</i>	



Andrijaitis Baltramiejus. Investigation of Robotic Incremental Formation of Polymer Sheet. Master's Final Degree Project, supervisor lect. Darius Eidukynas; Faculty of Mechanical Engineering and Design, Kaunas University of Technology.

Study field and area (study field group): Production and Manufacturing Engineering (E10), Engineering Sciences (E).

Keywords: Conduction, tool, incremental forming, simulation, formability, surface quality.

Kaunas, 2022. 61 p.

### **Summary**

Investigation of Robotic Incremental Forming of Polymer Sheet presents a work focused on increasing the process's quality. Increasing demand in high precision plastic parts and rapid prototyping industry growth brought to look for novel solutions. Literature analysis revealed formability and quality problems in the incremental forming process. A robotic incremental self-heating forming tool with a control system was designed as a possible solution. A few different experiments were performed to obtain experimental data. The applicability of a heating element was proved in experiments on temperature distributions in forming ball and polymer. The required power of the heater to maintain the best formability of plastic was found. During static and dynamic experimental research on the designed self-heating tool, capabilities of the tool and forming temperature boundaries were set. Obtained data were used in the development of simulation to research forming forces' influence on polymer. Final research on incremental sheet forming with a novel self-heating tool was performed to compare results with other studies' findings. Results of experiments were obtained through high precision multiple measuring. As a significant result, a direct dependency of process temperature on forming speed was presented. Findings revealed that an increase in a tool's diameter increases forming forces, and a decrease in forming speed decreases forming forces. Results were compared with other authors' research. Best formability was achieved with a 54,5 mm/s speed and 11 mm diameter sphere. Higher surface quality and lower forming forces were achieved compared to the approaches taken without additional heating. Low overall power consumption was presented and compared to the local heating approach. To increase formability, recommendations for further research were presented. The idea of a deeper investigation on temperature–formability and temperature–force dependencies was performed. A maximum formability experiment was offered to find occurring errors and identify causes. Provided findings revealed that an optimal ratio of forming temperatures, forces, and process temperature is required to achieve the best quality and formability.

Andrijaitis Baltramiejus. Polimero lakšto robotizuoto palaipsninio formavimo tyrimas. Magistro baigiamasis projektas, vadovas lekt. Darius Eidukynas; Kauno technologijos universitetas, Mechanikos inžinerijos ir dizaino fakultetas.

Studijų kryptis ir sritis (studijų krypčių grupė): Gamybos inžinerija (E10), Inžinerijos mokslai (E).

Reikšminiai žodžiai: Kondukcija, įrankis, palaipsninis formavimas, formuojamumas, paviršiaus kokybė.

Kaunas, 2022. 61 p.

## Santrauka

Robotizuoto palaipsninio polimero lakšto formavimo tyrimas yra orientuotas į proceso kokybės gerinimą. Didėjanti aukšto tikslumo polimero plastiko detalių paklausa ir poreikis greitai prototipuoti gaminius paskatino mokslininkus ieškoti inovatoriškų sprendimų. Darbe pristatyta literatūros analizė leido atskleisti formavimo problemas ir kokybės netikslumus laipsniško formavimo procese. Buvo sumodeliuotas robotizuotas savaimė įkaistantis formavimo įrankis, kaip, galimai, tinkantis sprendimas pagerinti gaminio kokybę. Kokybiniais duomenimis gauti buvo atlikti skirtingi eksperimentai. Temperatūrų pasiskirstymo formavimo šrate ir plastike eksperimento metu buvo įrodytas šildymo elemento tinkamumas tolimesniems tyrimams. Buvo atrasta įrankiui reikalinga galia palaikyti tinkamiausiai plastiko temperatūrai formuojant. Atliekant statinius ir dinامينius įrankio tyrimus buvo nustatytos įrankio galimybės ir formavimo temperatūros ribos. Bandymai parodė, kad temperatūros didinimas įrankyje padidina formuojamumą kelis kartus, o tinkamiausia temperatūra tolimesniems tyrimams yra nuo 75°C iki 100°C. Gauti duomenys buvo panaudoti kuriant modeliavimą, tiriant formavimo proceso jėgų įtaką polimerui. Simuliacijos skaičiavimai parodė panašius į eksperimentų rezultatus. Taip pat, buvo atliktas laipsniško lakšto formavimo su nauju savaimė įkaistančiu įrankiu tyrimas, siekiant palyginti rezultatus su kitų tyrimų išvadomis. Eksperimentų rezultatai buvo gauti atliekant didelio tikslumo matavimus kelis kartus juos kartojant. Kaip reikšmingas darbo rezultatas, buvo pateikta tiesioginė proceso temperatūros priklausomybė nuo formavimo greičio. Išvadose buvo nurodyta, kad padidėjus įrankio skersmeniui didėja formavimo jėgas, o sumažėjus formavimo greičiui, jos mažėja. Darbo svarumas buvo įrodytas palyginus rezultatus su kitų autorių atliktais tyrimais. Geriausias formuojamumas buvo pasiektas naudojant dvigubą greitį, naudojamą kitų autorių priartėjimuose. Rezultatai parodė, kad pasiekta aukštesnė paviršiaus kokybė ir mažesnės formavimo jėgos, lyginant su formavimu be papildomo kaitinimo. Mažas proceso energijos suvartojimas, lyginant su lokaliu viso lakšto šildymu, darbe pateikiamas kaip svarus privalumas, tik lyginant iš ekonominė, tiek iš ekologinės perspektyvos. Siekiant padidinti formuojamumą, buvo pateiktos rekomendacijos tolesniems tyrimams. Buvo nurodyta idėja, kad gilesnė temperatūros – formuojamumo ir temperatūros – jėgos priklausomybių analizė gali ženkliai pagerinti gaminio kokybę. Pasiūlytas maksimalaus formavimo sąlygų eksperimentas, siekiant iširti pasitaikančias geometrijos klaidas ir nustatyti priežastis. Pateikti rezultatai atskleidė, kad norint pasiekti geriausią kokybę ir formuojamumą, reikalingas optimaliausių formavimo temperatūrų, jėgų ir proceso temperatūrų santykis.

## Table of contents

<b>List of figures</b> .....	<b>8</b>
<b>List of tables</b> .....	<b>11</b>
<b>List of abbreviations and terms</b> .....	<b>12</b>
<b>Introduction</b> .....	<b>13</b>
<b>1. Literature Analysis</b> .....	<b>14</b>
1.1. Polymer Forming Methods.....	15
1.1.1. Vacuum Bag Forming Process .....	16
1.1.2. Autoclave Forming Process.....	17
1.1.3. Close Pressure Thermoforming Process.....	18
1.1.4. 3D Printing .....	19
1.1.5. Injection Molding Process .....	21
1.2. Robotic Incremental Polymer Sheet Forming .....	22
1.2.1. Single Point Incremental Forming.....	22
1.2.2. Two-point Incremental Forming .....	24
1.3. ISPF Tools And Heating Possibilities .....	25
1.3.1. Glass Transition Temperature .....	25
1.3.2. Polymer Heating Methods .....	26
1.3.3. ISPF Tool Patents .....	27
<b>2. SPIF Self-heating Tool Design</b> .....	<b>30</b>
2.1. Heating Control System .....	30
2.2. Heating Process Investigation .....	32
2.3. Design of SPIF Self-heating Tool .....	36
<b>3. Experimental Research of Self-heating Forming Tool</b> .....	<b>37</b>
3.1. Static Experiment of a Self-heating Forming Tool .....	37
3.2. Dynamic Experiment of a Self-heating Forming Tool.....	41
<b>4. Simulation of Forming Forces on a Polymer Sheet</b> .....	<b>46</b>
4.1. Thermal Simulation of Temperature Distribution .....	46
4.2. Static Structural Simulation of Forming Forces .....	48
<b>5. Robotic Incremental Forming of Polymer Sheet</b> .....	<b>51</b>
5.1. Experimental Background .....	51
5.2. Results of Robotic Incremental Forming Approach.....	53
5.2.1. Formability .....	53
5.2.2. Quality .....	55
<b>Conclusions</b> .....	<b>57</b>
<b>Recommendations</b> .....	<b>58</b>
<b>List of references</b> .....	<b>59</b>

## List of figures

<b>Fig. 1.</b> Working principle of vacuum bag forming process [8].....	16
<b>Fig. 2.</b> Autoclave forming process model [10].....	17
<b>Fig. 3.</b> Working principle of autoclave forming process [10].....	17
<b>Fig. 4.</b> Working principle of close pressure thermoforming process. a) heating; b) sealing; c) forming and cooling; d) removing [12].....	18
<b>Fig. 5.</b> SLA printing technology (left) and CLIP printing technology (right) [13].....	19
<b>Fig. 6.</b> SLS printing technology (left) and FFF printing technology (right) [13].....	20
<b>Fig. 7.</b> Multi-jet printing technology [13].....	21
<b>Fig. 8.</b> Working principle of an injection molding process [14].....	21
<b>Fig. 9.</b> Process of SPIF: 1 – frame, 2 – forming tool, 3 – clampings, 4 – polymer sheet [15].....	22
<b>Fig. 10.</b> Main types of SPIF tools. $R$ – radius of the tool, $r$ – radius of fillet [16].....	23
<b>Fig. 11.</b> Main toolpath strategies for ISPF process: a) parallel, upgrading, b) parallel, downgrading, c) zigzag, continuous [15].....	23
<b>Fig. 12.</b> Process of TPIF with a partial die [18].....	24
<b>Fig. 13.</b> Process of DSIF with a counter tool [19].....	24
<b>Fig. 14.</b> The forming strategies of DSIF [15].....	25
<b>Fig. 15.</b> Continuous polymer electromagnetic induction welding robot [21].....	26
<b>Fig. 16.</b> Simplified structure diagram of ultrasonic incremental sheet polymer forming tool [25] ..	28
<b>Fig. 17.</b> Working principle of the patent's US 8,033,151 forming tool, 406, 426, 436 – stylus, 408 – forming tool, 412 – sheet part, 430 – ultrasonic energy, 432 – an area of energy impact, 434 – location of boundaries, 438 – applied forming force [24].....	28
<b>Fig. 18.</b> Working principle of single-point tool forming patent US 7,984,635. 1 – sheet material, 2 – clamping system, 3 – forming tool, 4 – heating system, 5 – heat flux, 6 – cooling system, 8 – synchronization controller [27].....	29
<b>Fig. 19.</b> The concept of SPIF self-heating tool: 1 – clamping, 2 – sheet, 3 – forming ball, 4 – tool, 5 – heating element, 6 – 6-axis robot hand, 7 – thermal sensor, 8 – heat control system.....	30
<b>Fig. 20.</b> 60W soldering-iron heat element used in the investigation of incremental process.....	31
<b>Fig. 21.</b> Heating control system elements: REX-C100 48x48 AC 100-240V thermocouple RTD Input Digital PID Temperature Controller [28] (left). Thermocouple sensors K-type 0-800C [29] (right).....	31
<b>Fig. 22.</b> Wiring scheme of a heating control system. 1 – Forming tool, 2 – 60W soldering-iron heat element, 3 – Solid-state relay (SSR), 4 – PID temperature controller, 5 – thermocouple, 6 – AC power supply.....	31
<b>Fig. 23.</b> The experimental calibration scheme (left) and set-up view (right). 1 – DC Power Supply HY1803D (0-18V, 3A), 2 – Stand, 3 – Clamp, 4 – Heater with magnet and ball, 5 – Thermocouple, 6 – Digital Multimeter UNI-T UT161D, 7 – PC.....	32
<b>Fig. 24.</b> Scheme of heater construction of carried research (left) and setup view (right). 1 – ball, 2 – magnet, 3 – heating element, 60W 4 – textolite STAF-1 plates, 5 – clamping, 6 – thermocouple... ..	33
<b>Fig. 25.</b> Temperature values of $\varnothing 12,5$ mm sphere under different power versus time.....	33
<b>Fig. 26.</b> Scheme of polymer's heating investigation (left) and setup view (right). 1 – DC Power Supply HY1803D (0-18V, 3A), 2, 4 – Stands, 3 – Digital Multimeter CHY 24CS LCR METER, 4 – Heater with magnet and ball, 5 – Clamp, 6 – Sample, 7 – PC, 8 – Heating element, 9 – Digital Multimeter UNI-T UT161D.....	34

<b>Fig. 27.</b> A view of held investigation's schematic (left) and experimental setup (right). 1 – Stand, 2 – Sample, 3 – Thermocouple, 4 – Forming ball, 5 – Textolite STAF-1 plates, 6 – Heating element, 7 – Clamp .....	34
<b>Fig. 28.</b> Temperature values of sheet layers under different forming ball temperatures versus thickness of a sheet.....	35
<b>Fig. 29.</b> Temperature values of sheet layers under 75°C forming ball temperature versus time .....	35
<b>Fig. 30.</b> Designed SPIF self-heating tool. 1 – Heating element, 2 – magnet, 3 – forming ball, 4 – tool, 5, 6 – bushings.....	36
<b>Fig. 31.</b> Schematic view of static self-heating forming tool experiment (left), setup view (right). 1. – DC Power Supply HY1803D (Mastech Digital, Inc., USA), 2 – FCS-C series platform scales (UAB Mingeda, Lithuania), 3 – Praktika drilling machine TU2-024-2546-70, 4 – Designed SPIF self-heating tool, 5 – PVC ESA-D 3mm thickness polymer sheet.....	37
<b>Fig. 32.</b> Samples after the static experimental research: 1. – Sphere Ø12,5mm, 50°C, 2. – Sphere Ø12,5mm, 75°C, 3 – Sphere Ø12,5mm, 100°C, 4. – Sphere Ø11mm, 50°C, 5. – Sphere Ø11mm, 75°C, 6. – Sphere Ø11mm, 100°C .....	38
<b>Fig. 33.</b> The principle of the static experiment: 1 – hot sphere, 2 – sample, $F$ – initial force, $F_{60}$ – reduced force after 60 seconds of deformation, $h$ – depth of the imprint, $d_I$ – diameter of the imprint .....	38
<b>Fig. 34.</b> Incremental sheet forming quality dependence on step size. The thickness of the sheet – 12mm [33] .....	39
<b>Fig. 35.</b> Set-up schematic view of static experiment result measurements (left), set-up view (right). 1. – Stand, 2 – Keyence Display panel (Keyence, Inc., USA), 3 – Magnets, 4 – Sample, 5 – High speed, high accuracy CCD Laser Displacement Sensor (Keyence, Inc., USA).....	39
<b>Fig. 36.</b> Depth of imprint values under different forming ball diameters and temperatures versus applied forces.....	40
<b>Fig. 37.</b> Set-up schematic view for dynamic self-heating forming tool experiment (left), set-up view (right). 1. – Manipulator ABB IRB1200 (ABB Robotics & Discrete Automation, Västerås, Sweden), 2 – Designed SPIF self-heating tool, 3 – PVC ESA-D 3mm thickness polymer sheet, 4 – DC Power Supply HY1803D (Mastech Digital, Inc., USA), 5 – Digital Multimeter (Uni-Trend Technology Co., Ltd., China), 6 – FCS-C series platform scales (UAB Mingeda, Lithuania), 7 – Holding frame .....	42
<b>Fig. 38.</b> Samples after the dynamic investigation .....	43
<b>Fig. 39.</b> The principle of the dynamic experiment: 1 – hot sphere, 2 – sample, $F$ – initial force, $h$ – speed of moving sphere, $h$ – depth of the groove, $d$ – width of the groove .....	43
<b>Fig. 40.</b> Set-up schematic view of dynamic experiment result measurements (left), set-up view (right). 1. – Stand, 2 – Keyence Display panel (Keyence, Inc., USA), 3 – Magnets, 4 – Sample, 5 – High speed, high accuracy CCD Laser Displacement Sensor (Keyence, Inc., USA).....	43
<b>Fig. 41.</b> Depth of groove values under different forming ball diameters and temperatures versus applied forces.....	44
<b>Fig. 42.</b> Properties of PVC Trovidurv ESA-D material in ANSYS Library .....	46
<b>Fig. 43.</b> Initial conditions of thermal simulation .....	47
<b>Fig. 44.</b> Quad Hex Dominant mesh with a size of single element size of 0,25 mm .....	47
<b>Fig. 45.</b> Temperature distribution in a sheet while affected with 75°C forming ball: a) top view, b) front view.....	48
<b>Fig. 46.</b> Simulated temperature values of sheet layers under different forming ball temperatures versus thickness of a sheet.....	48
<b>Fig. 47.</b> Initial conditions of static structural simulation.....	49

<b>Fig. 48.</b> Quad Hex Dominant mesh with a size of single element size of 0,2 mm .....	49
<b>Fig. 49.</b> Displacements of the sheet while affected with 75°C forming ball and 300N force: <i>a)</i> top view, <i>b)</i> front view .....	50
<b>Fig. 50.</b> Simulated depth of imprint values under 12,5 mm forming ball diameter and different temperatures versus applied forces .....	50
<b>Fig. 51.</b> Essence of held incremental forming process and main variables: $\Delta z = 0,5$ mm, $\Delta y = 0,5$ mm, $d_{RT} = 12,5$ mm and 11 mm, $\alpha = 45^\circ$ , $h = 30$ mm [36] .....	51
<b>Fig. 52.</b> Process investigation schematic view (left), set-up view (right). 1. – Manipulator ABB IRB1200 (ABB Robotics & Discrete Automation, Västerås, Sweden), 2 – Thermal imaging camera FLIR T450sc (Teledyne FLIR LLC, USA), 3 – DC Power Supply HY1803D (Mastech Digital, Inc., USA), 4 – PVC ESA-D 2mm thickness polymer sheet, 5 – Digital Multimeter (Uni-Trend Technology Co., Ltd., China), 6 – Designed SPIF self-heating tool, 7 – Holding frame, 8 – FCS-C series platform scales (UAB Mingeda, Lithuania) .....	52
<b>Fig. 53.</b> Samples after the SPIF process: 1. Ball diameter 12,5 mm, feed rate 73 mm/s, lubricant – none, 2. Ball diameter 11 mm, feed rate 54,5 mm/s, lubricant – none, 3. Ball diameter 11 mm, feed rate 18,3 mm/s, lubricant – none 4. Ball diameter 11 mm, feed rate 73 mm/s, lubricant – motor oil	53
<b>Fig. 54.</b> Data acquired through thermal imaging camera FLIR T450sc. Feed rate 18,3 mm/s., 44,7°C (left), feed rate 73 mm/s., 51,7°C (right) .....	53
<b>Fig. 55.</b> Polymer’s surface temperature dependence on feed rate .....	54
<b>Fig. 56.</b> Forming force dependence on feed rate under same initial conditions .....	54
<b>Fig. 57.</b> Formed height of part dependence on feed rate under same initial conditions with $\varnothing 11$ mm forming ball .....	55
<b>Fig. 58.</b> Set-up schematic view of surface roughness measurements (left), set-up view (right). 1. – Clamp, 2 – Formed part, 3 – Roughness tester with graphical display TR220 (Beijing TIME High Technology Ltd., South Korea), 4 – Clamp, 5 – Stand, 6 – Magnet .....	55

## List of tables

<b>Table 1.</b> Polymers with their thermal properties [20] .....	26
<b>Table 2.</b> Results of the static experiment with a self-heating forming tool .....	40
<b>Table 3.</b> Results of the dynamic experiment with a self-heating forming tool.....	44
<b>Table 4.</b> Properties of PVC Trovidurv ESA-D polymer material.....	46
<b>Table 5.</b> Initial conditions of a held experiment .....	52
<b>Table 6.</b> Measured values of surface roughness under different experimental conditions .....	56

## **List of abbreviations and terms**

### **Abbreviations:**

ISPF – incremental sheet polymer forming

ISF – incremental sheet forming

SLA – stereolithographic

CLIP – continuous liquid interface production

SLS – selective laser sintering

FFF – fused filament fabrication

SPIF – single point incremental forming

TPIF – two-point incremental forming

DSIF – dual side incremental forming

PID – proportional, integral, derivative

SSR – solid state relay

PVC – polyvinylchloride



## Introduction

Globalization and the rapid evolution of industry shapes fast-moving world where every person is able to live a comfortable and enjoyable life. Improving living conditions, growing needs of daily commodities, and increasing complications of technologies increase demands in custom and fast made production, flexible and adaptive manufacturing. Emerging Industry 4.0 revolution allows controlling manufacturing chains while automating autonomous machines, advanced robots, creating AI and learning machines. The fourth industrial revolution allows achieving automation which increases the efficiency and capability of manufacturing. One of many perspective automated manufacturing fields affected by the revolution is plastic processing. Plastic variety and applicability are increasing exponentially due to the possibility of altering their characteristics and properties. Increasing custom needs, requirements of products, and new plastics applications force scientists to research novel robotic methods and manufacturing possibilities. One of them is automated incremental sheet polymer forming (ISPF). The incremental sheet polymer forming process usually consists of a 6-axis robot or CNC machine with a single point forming tool that gradually increments the plastic. This flexible method of stamping has the potential to create different geometry low volume plastic sheet products with high quality and low manufacturing price compared to 3D printing or different stamping processes such as die stamping, deep draw, and roll forming. This novel process does not require any stamps or dies and can be easily reprogrammable for different shapes without losing the usability of equipment. Incremental sheet polymer forming has the potential to reduce manufacturing costs and time in aircraft, biomedical, automotive, military, and prototyping industries.

The requirements of the ability to adapt the process and machine to constantly changing demands and the possibility to rapid prototype make a unique opportunity for robotic ISPF to become a leading plastics stamping process in the future. However, due to the novelty of the technology in plastic manufacturing, the process must be investigated more consistently. Lack of quality, inaccuracy of geometries, and errors such as wrinkles, cracks, spring backs, and voids prevent technology from achieving comprehensive employment in industries. Investigations of variables such as spindle speed, step size, forces, the thickness of the sheet, and effects such as local heating, sonic vibrations, and material characteristics that influence process quality justify the lack of research and demand deeper analysis. The aim of this work is to investigate robotic incremental sheet polymer forming, proposing a novel approach to improve the process and applicability. A self-heating forming tool for ISPF will be presented as a possible solution that could improve the quality of the formed sheet and reduce forming energy consumption. To approve or deny this hypothesis main few tasks of this work must be fulfilled. Firstly, a self-heating tool for the process must be designed. The tool must maintain the temperature most suitable for the polymer's best possible processing quality. Simulation of forming forces and experiment of designed tool incremental forming must be held to investigate the influence of the novel approach.

Aim: To investigate the incremental forming of polymer sheets using a single point heating tool.

Tasks:

1. To design a self-heating forming tool for incremental single point forming.
2. To conduct experimental research on the designed self-heated tool.
3. To make a simulation of heated tool incremental forming forces on polymer sheet.
4. To perform robotic incremental forming of polymer sheet using developed single point heating tool.

## 1. Literature Analysis

Incremental sheet forming (ISF) technology is a suitable and flexible solution to create complex 3D geometries of the sheet. A sheet is gradually formed into the desired shape with a forming tool usually attached to a CNC machine or robot. Small deformations are made on the blank each time the position of the tool incrementally downgrades. This process is valid with metal as well as with polymer sheets. Incremental sheet forming has a vast potential in rapid prototyping and small-batch manufacturing [1]. CNC or manipulator can be easily reprogrammable to execute a different program for different geometry of the blank. It is essential to mention that this process does not require any stamps and dies, which makes ISF economically attractive as a solution. The absence of casting dies and specialized tools reduces time consumption and costs of the final product or prototype [1]. As the demand for custom orders and prototyping requirements increase, incremental sheet forming becomes a relevant technology that expands the possibilities of traditional sheet forming technologies and applications. ISF technology has the potential to replace some 3D printing processes since there is no support material needed in incremental sheet forming, and forming time is shorter compared to 3D printing. More complicated geometries are formed with ISF technology. 3D printers have a limited printing area. The process has become relevant in the automotive, aircraft, aerospace, and biomedical industries. As technologies advance, the automotive industry requires more complex and high-precision geometries of sheet products [2]. Incremental sheet forming technology can manufacture lightweight asymmetric products that are ideal for automotive applications. Reducing the mass of the components leads to a decrease in energy consumption and CO<sub>2</sub> reduction [3]. Increasing demand for electric cars creates a demand for new lightweight parts of the vehicles, which must be made out of low thickness plastics and composites. New demand creates a problem where deep drawing or stamping is inefficient with new materials. Application of ISF in the automotive industry reduces the investments for dies and punch, which are no longer needed to create desired shape components. Even if this novel technology is used only for prototyping and testing in the automotive industry, it saves time and reduces costs due to the high costs of dies and punches [2]. Other industries where incremental sheet forming can become a crucial process are aircraft and aerospace. Since aircraft must be immune to temperature changes, oxidation, and strong enough to withstand bird collisions, materials like polymers are becoming essential in this industry. Polymer sheets possess characteristics to withstand increased temperatures and collisions with birds, and these parameters make incremental sheet forming even more appropriate in this industry. ISF has the potential to reduce costs, manufacturing time and increase the flexibility of geometries in aircraft and aerospace industries [4]. The process not only reduces economic obstacles but also decreases pollution. With the ability to reduce the mass of lightweight aircraft components and the automotive industry, less energy is wasted, and higher CO<sub>2</sub> reduction is achieved. Rapid prototyping also can be used successfully in this industry. It reduces time and costs consumptions while allowing to renounce expensive dies and presses and their crafting. Biomedicine is another industry where incremental sheet forming has tremendous potential. Implants and prostheses require high geometrical accuracy and are mostly customized for small batch production in the biomedicine field [5]. The main application of ISF technology can be components such as ankle prostheses, cranial implants, knee prostheses, and various biomedical devices [6]. Since every patient is unique in their anatomy, only custom-made implants can be applied. Stamps and dies are not the solution due to high costs and low flexibility. ISF technology is a new possibility and hope for thousands of patients who require complex and high precision geometry solutions. Moreover, as in other industries, incremental sheet forming allows

rapid prototyping of prostheses and implants to create accurate profiles that ensure biocompatibility [7].

However, the inaccuracy of geometry and occurring process errors in previously discussed industries prove the novelty of the technology. Previous investigations [1] confirm that ISF is still hardly employed in manufacturing sectors due to the lack of understanding of the process and knowledge on improving precision and reducing surface roughness. The majority of research focuses on the parameters such as a spindle feed rate, a tool diameter, and a step size to find a dependency between the values and output of the forming [1] without considering heating as a friction-reducing and formability increase solution. The automotive industry requires various wall angles, thickness of walls, accuracy, and forming limits. Research with different materials, sheet thickness, and forms was examined to achieve valid parameters [2], again, without considering tool influence and local heating to reveal stresses. Occurring cracks, inclusions, and wrinkles detain ISF technology from dominating the automotive industry. As well as automotive industry, the aerospace and aircraft industry require high precision and complex geometries. Incremental sheet forming technology research in this manufacturing section proves novelty due to the inability to use the full potential of the process. Recent works show the forming of polymer aircraft parts where the tool's rotation speed and toolpath were investigated. Results [4] revealed that surface quality and deviation of some samples were in the allowable range with specific parameters, however, the lack of ISF research limits applications in the aircraft industry. The novelty of incremental sheet forming and tool heating can be observed in the research on process applicability for biomedicine. Published novel research [5] focuses on implant forming while investigating friction, forces, and toolpath dependence on geometry accuracy. Another research on ISF in the biomedical industry states that the technology still has difficulties being applied widely despite the progress. The combination of various parameters such as wall thickness, a blank size, a wall angle, geometries, and material characteristics creates a significant problem in acquiring precise geometries [6]. Moreover, errors like wrinkles and spring backs must be solved to apply the process in biomedicine. However, no tool heating investigations were performed to find a dependency between the self-heating tool and the quality of the blank.

The relevance and novelty of incremental sheet forming technology prove that more research must be performed to find a solution to improve the quality of the process and reduce energy consumption. A deeper literature analysis must be conducted to fully understand the processes and fulfil the project's tasks. Further in this chapter, three main sections of the analysis are presented where polymer forming methods, robotic polymer sheet forming, incremental sheet forming tools, and heating possibilities of the sheet and tool are discussed.

### **1.1. Polymer Forming Methods**

Polymer forming methods must be researched to understand polymers' characteristics and their forming possibilities. The lack of ISPF processing precision and effectiveness requires a more profound analysis of other forming technologies, emphasizing advantages and disadvantages. This section presents the primary polymer forming methods: vacuum bag forming, autoclave forming, close pressure thermoforming, 3D printing, and injection molding, and provides working principles with the effect analysis on polymer materials.

### 1.1.1. Vacuum Bag Forming Process

One of the modern polymer forming methods is the vacuum bag forming process. Technology's flexibility allows forming a wide range of shapes and different sizes of laminates. It is a feasible solution for forming low viscosity polymers. However, more research must be done to apply the process on high viscosity sheets [8]. The working principle of the vacuum bag forming process is shown in Fig. 1. Material with its layers is shaped in mold and placed in an oven on a tooling base. The material comprises a few main layers needed for a splendid process: the material to be consolidated, the peel ply, which increases surface finish and demolding, and the breather felt to provide an escape route for air to reduce voids. Mold is covered with a vacuum bag which is sealed with sealant tape. Air is removed from the mold via a vacuum source channel with the vacuum pump, and atmospheric pressure is applied to the system. The oven's temperature depends on the composites' constitution used in the material. Atmospheric pressure and temperature form the sheet in the form of mold. Once the sample is solidated, pressure is released, peel ply can be removed, and the part removed from the oven.

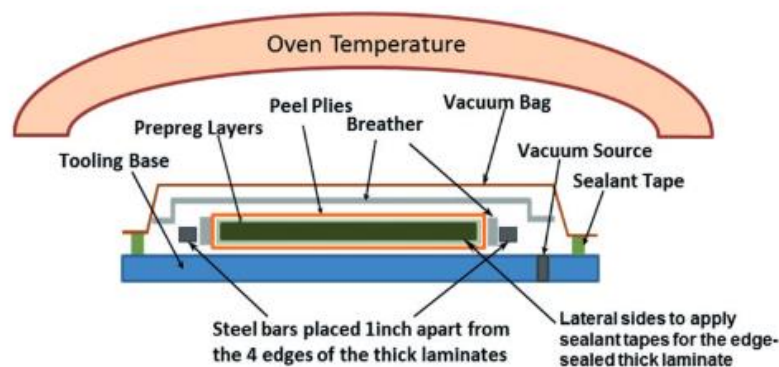


**Fig. 1.** Working principle of vacuum bag forming process [8]

This technology has low manufacturing costs compared to other methods like autoclave forming [8]. Low atmospheric pressure reduces the tooling cost of the process. However, this process has a high void error risk (5% – 10%) [8]. Consolidation pressure is lower compared to processes such as autoclaving. These disadvantages lead to reduced quality and performance of the part. Void occurrence and dimensional nonuniformity in this process are the main drawbacks of the technology. Voids negatively affect the mechanical characteristics and reduce the lifespan of polymers. Void occurrence depends on variables such as the thickness of a sheet, geometry complexity of the mold, used materials, and pressure distribution [9]. However, the deviation of error can be reduced by applying defect reduction strategies. Intermediate debulking removes air trapped between the layers. An increase of form corner radiuses reduces the potential of resin accumulation. The concentration of pressure in corners and radiuses increases the quality of the process [9]. Another limitation is the ecology of this technology. It generates much waste, such as vacuum bags, breather fabric, and peel ply, which must be discarded after the forming [8]. Mold can not be used to form differently shaped samples, and as a result, rapid prototyping and small-batch production are expensive. Only one side of the sample acquires desired surface quality in the process.

### 1.1.2. Autoclave Forming Process

Another applicable polymer forming method is the autoclave forming process. This popular method has a high performance and precision compared to similar technologies such as closed pressure forming. The process is compatible with advanced polymer materials and is applicable to manufacturing large products. As in the vacuum bag forming technology, the temperature of the autoclave process is an essential factor in achieving precision. As the mold size increases, it is more challenging to ensure uniform temperature distribution. As shown in Fig. 2, the process model mainly includes fan, heat source, pressure system, pressure vessel, stage, slideways, control, and vacuum systems.

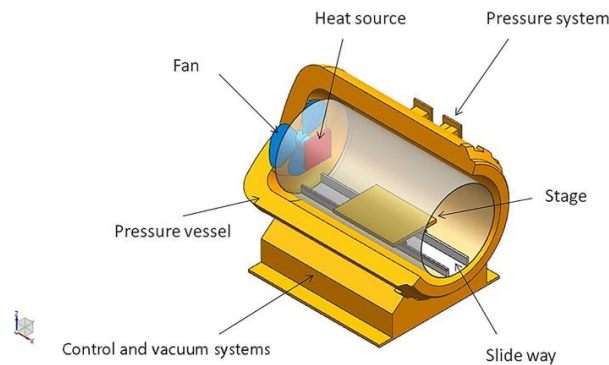


**Fig. 2.** Autoclave forming process model [10]

The working principle of technology is shown in Fig. 3. In this process heating source heats the fluid (usually air), and the fan is used to cycle fluid in the chamber. Three main heat transfer methods apply in the process: conduction, convection, and radiation. However, radiation is only applied when the system's temperature exceeds 180 °C [10]. As the air is heated in the chamber, temperature changes the mold's frame structure. Autoclave allows to change the pressure and control needed parameters inside the chamber.

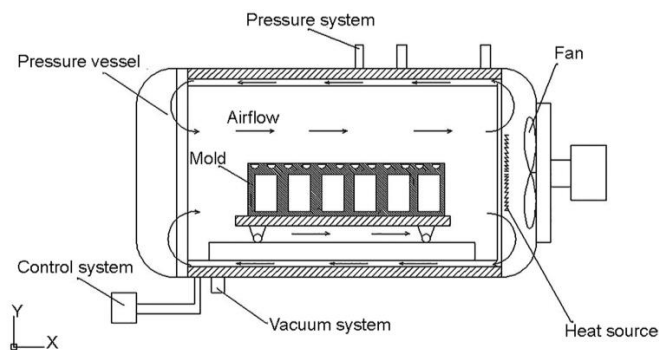


**Fig. 3.** Working principle of autoclave forming process [10]

This forming technology has higher manufacturing costs than most other forming processes but has high precision and no limitations in form dimensions. One of the main advantages of this process is the absence of void occurrence due to the vacuum system. The technique is popular in manufacturing, where parts need a high strength-to-weight ratio. The unique performance allowed this technology to advance in many industries such as aviation and biomedicine. However, the sensitivity of pressure and uniform temperature distribution makes the process hard to use widely in manufacturing. Usage of mold increases manufacturing costs in small-batch and rapid prototyping industries.

### 1.1.3. Close Pressure Thermoforming Process

The potential polymer forming method is close pressure thermoforming process. This technology is the widely applicable polymer processing method due to low manufacturing costs and high process rates. The thermoforming technique is a temperature-based process where the solid-state sheet is turned into a soft state and deformed in sequence. Process temperature of the system is the most critical parameter. It affects mechanical properties and the quality of surfaces [11]. Overheating polymer sheet leads to uneven deformations and deterioration of surface finish – air bubbles. An ideal temperature for processing polymers is Glass transition temperature ( $T_g$ ) [11]. This point is achieved in the time interval when the polymer is changing its state from solid to soft. Since every polymer has different material characteristics, the value of every polymer's  $T_g$  temperature varies. Without this parameter, deformation pressure and plug displacement are influential variables to the quality.

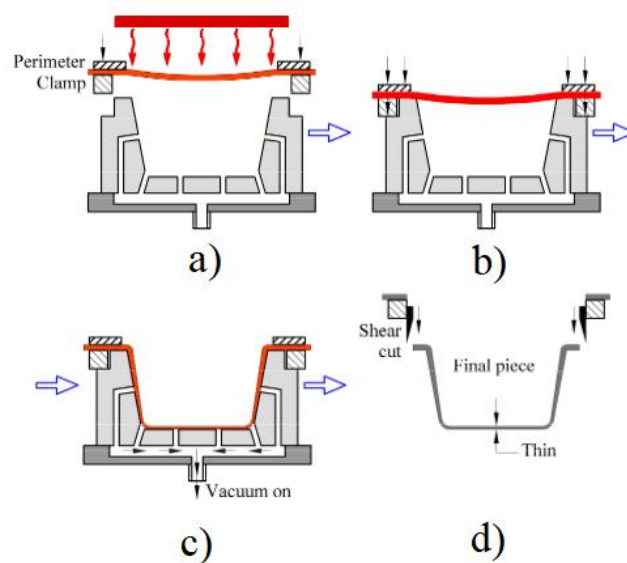


**Fig. 4.** Working principle of close pressure thermoforming process. a) heating; b) sealing; c) forming and cooling; d) removing [12]

Three main types of thermoforming technology are pressure, vacuum, and contact. The technology consists of three main steps: heating, forming, and cooling. The working principle of close pressure vacuum thermoforming is shown in Fig. 4. Firstly, the sheet is clamped and sealed to the mold. In sequence, heat is transferred through the air into the chamber and heats the solid polymer sheet into soft and formable till the temperature of  $T_g$  is reached. The vacuum system creates negative pressure that forms the sheet by “pulling” it to the mold walls. When the sample is cooled down, it can be removed from the mold. The process applies to serial production due to the high processing rate. Technology can achieve high precision with the required amount of heat. There are several disadvantages of the process. Difficulties in finding Glass transition temperature prevent technology from dominating manufacturing. Due to the usage of mold and incurring costs, the process can not be applied in small-batch production and rapid prototyping. Also, the technique is limited in processing higher thickness samples and achieving complex geometries, and parts might require post-processing.

### 1.1.4. 3D Printing

Another technology widely used in polymer forming industries is 3D printing. Due to the early additive manufacturing equipment patent expiration, 3D printing is widely used in industry and the general public. There are three main production types of 3D manufacturing: forming, subtractive and additive manufacturing. Forming is a process where a part is shaped without adding or subtracting any material. Subtractive production – part is shaped by reducing the mass of the material by removing it. Additive manufacturing excels in adding material to the part to shape it the way it is needed. The additive process has few advantages over others. Firstly, technology allows shaping complex geometry almost without any constraints. However, with more complex geometry, more supporting material might need. 3D printing is also known as a technique perfect for rapid prototyping. This process allows efficiently converting models from software to physical bodies. As 3D printing developed, a new language of file reading appeared. Standard Tessellation Language allows to create a visualization of printable parts and slice it to the layers of the printer step. This printing process uses polymer powders, filament, and sometimes photosensitive resins. There are a few leading 3D printing technologies: stereolithographic (SLA), continuous liquid interface production (CLIP), selective laser sintering (SLS), fused filament fabrication (FFF), and multi-jet printing [13].

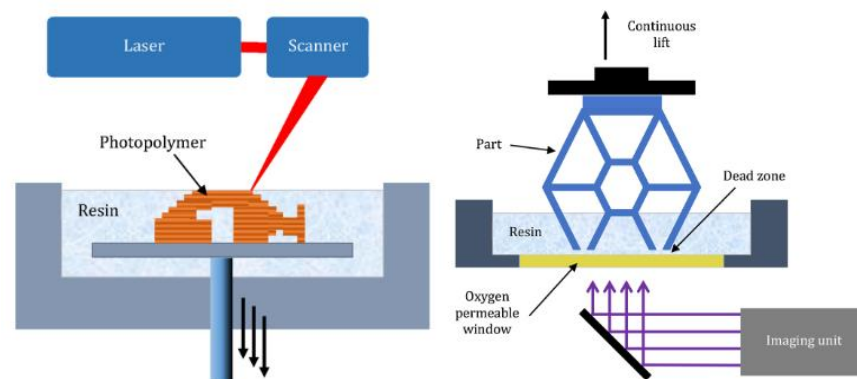


**Fig. 5.** SLA printing technology (left) and CLIP printing technology (right) [13]

The main working principle of SLA printing technology is shown in Fig. 5. This process uses photosensitive liquid resin exposed to a UV laser. The depth of the liquid level determines the height of the part. The laser with a scanner can move in the X and Z axis while the table with the part moves in the Y-axis downgrading by the step of printer's nozzle between 50 and 200  $\mu\text{m}$  into the resin [5]. The movement is determined by the photo-initiator, conditions such as wavelength, power and exposure velocity, dyes, pigments, and other UV absorbers. Absorbers allow the technology to print transparent parts. However, the process using a near-IR laser can achieve the step of 10  $\mu\text{m}$ . When the printing is done, the resin is drained and can be used in future printing. Part is cleaned from resin and supporting material.

Another very similar printing technology is the CLIP process. A schematic view of the CLIP working principle is shown in Fig. 5. This technology uses a bottom-up building approach facilitated through well-controlled oxygen inhibited dead-zone that avoids attachment of the part to an oxygen-permeable curing window [13]. The window has a low reflection of light and high optical clarity. The imaging unit can move in the X and Z axis while the table with the part moves upwards in the Y-axis. Differently, as in SLA technology, viscosity is a crucial part of reaching the best quality and



mechanical characteristics there. The printing speed of the device is up to 1000 mm/min and depends on the rate of resin replenishment, area of light exposure, and the composition of the liquid [13].

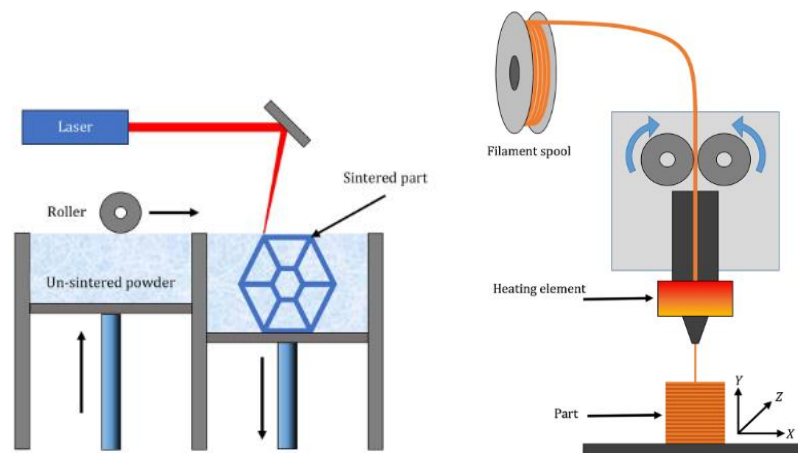


**Fig. 6.** SLS printing technology (left) and FFF printing technology (right) [13]

SLS printing technology uses semi-crystalline thermoplastic polymer. This technology is based on preheating polymer close to liquid form temperature, which is needed to awake crystallization of polymer in the cooling process. The working principle of this process is shown in Fig. 6. Lever with un-sintered powder moves upwards while roller moves the powder to the printing area. Particles are sintered with the laser, which inputs a high-power CO<sub>2</sub> beam. The laser fuses particles into the layer of printing. The layer thickness is equal to 30 – 90 μm due to the size of the polymer particles. Bed with sintered parts is moving downwards in Y-axis by the step size of the printer. The laser's power, beam speed, and spacing between scans must be monitored closely to reach the best quality of the part.

Another technology that is widely used by the general public is the FFF printing process. This technique, as well as SLS printing, uses polymer powder. Despite the similarity, this process melts the powder before the process and feeds material through the nozzle. The scheme of the working principle is shown in Fig. 6. The printing head can move up and down in Y-axis and has a heating element that melts the polymer. The process's ionizing radiation converts a thermopolymer into a thermoset printed part while increasing mechanical properties and solvent resistance. However, colors can not be mixed as in the multi-jet process. Technology can attach several printing heads that allow printing with different materials, supports, or complex overhanging geometries. Due to the high tolerance of heating, the process has the widest variety of polymers in the FFF technique. Recycled polymers can be used as well.

Multi-jet printing technology is applicable to print high surface quality and complex parts. This process allows achieving the layer size below 20 μm [13]. The working principle of the technique is shown in Fig. 7. Multi-jet printing allows using several printing heads at a time, so photopolymer can be applied where needed. Since several printing heads can be used, different colors, characteristics of materials, materials, and supports can be used in the printing. Inject heads with curing light source and leveling blade can move in the X and Z axis while the table with the part moves upwards and downwards in the Y-axis. Leveling blade is used to ensure uniformity of layers before affecting them with the curing light.



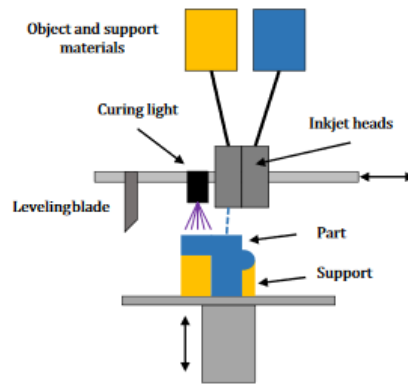


**Fig. 7.** Multi-jet printing technology [13]

Despite all the advantages of 3D printing, there are some drawbacks, such as limited printing materials and restricted building size, defined by printed, more significant printers requiring more capital. Mostly printed parts require post-processing, and while parts are printed layer-by-layer, there is a possibility of delamination due to stress and fatigue.

### 1.1.5. Injection Molding Process

Injection molding is a rapidly growing technology and a popular solution for new applications in the automotive, electronics, and medical industries. The technique is becoming one of the most applicable methods in polymer processing due to the quality of part and cost ratio. There are three main stages in injection molding. The filling is the process where the molten polymer is injected into the mold. The packing process traps molten polymer in the mold and prevents it from shrinking. Cooling is the last stage and ensures cooling of the part before ejecting. The working principle of the injection molding process is shown in Fig. 8.

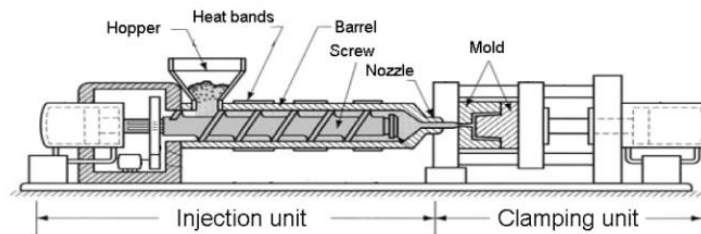


**Fig. 8.** Working principle of an injection molding process [14]

Hopper contains polymer granules and feeds to the screw. The rotating screw transports material through the injection unit. The velocity of the feed is an influential parameter in the technique. In the process, heat bands melt the polymer granules. Temperature is one of the most relevant parameters. Heating bands are set to different temperatures, which are increased by advancing in the barrel. Through the nozzle, molten polymer is fed to the mold. Created pressure in the mold is an essential parameter to the quality and, together with temperature, is called  $pV_T$  relationship [14]. The quality of a part also depends on the geometry complexity of the mold. Cooling is necessary in order to reach needed mechanical properties. Cooling is a complex process where shrinkage and heat conduction must be considered. Moreover, after removing the part, it cools at room temperature. It can affect the quality of the part. Despite the advantages such as precision, low cost, material possibilities, and repeatability, the process has a high tooling and machinery cost. Technology has geometry and size limitations of parts and is not applicable in rapid prototyping and small-batch production.

## 1.2. Robotic Incremental Polymer Sheet Forming

As the Industry 4.0 revolution emerged, robots and automation possibilities significantly increased the efficiency and capability of manufacturing. To research novel incremental forming methods, robotic systems must be studied. Automated polymer sheet forming methods must be researched to obtain knowledge of the most appealing incremental forming processes. Robotic solutions must be flexible to adjust in rapid prototyping, small-batch manufacturing and achieve efficiency in processing. A profound analysis of the leading robotic incremental polymer sheet forming must be conducted to determine the advantages, disadvantages, and factors influencing the outcome of the process.

### 1.2.1. Single Point Incremental Forming

One of the most advanced automated polymer sheet forming methods is single point incremental forming (SPIF). Machine programming and forming path creation on CAD allows technology to achieve high efficiency in rapid prototyping and small-batch manufacturing. SPIF has high formability limits and has the potential to achieve high-quality production. This method also has advantages over methods such as spinning, stamping, drawing, and molding of the possibility to form asymmetric parts and no requirement of dies or different tools [15]. The forming process contains two contacts: the forming tool and polymer blank and another between clamps and polymer sheet. CNC machines, purpose-built machines, robots, or hexapods with a forming tool designed with force, pressure or temperature sensors to follow the generated path while forming the blank. The process of incremental sheet forming is shown in Fig. 9.

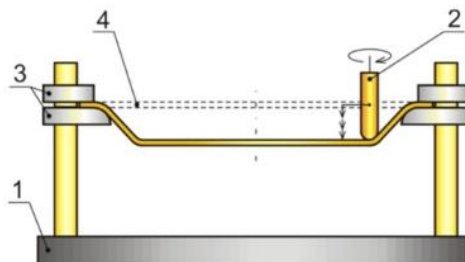


**Fig. 9.** Process of SPIF: 1 – frame, 2 – forming tool, 3 – clampings, 4 – polymer sheet [15]

SPIF process can form various metals, polymer sheets, and sandwich panels. However, this process is still being studied due to the complexity of dependent variables and temperature, spring back, and deformation mechanisms. Material, tool, toolpath, and geometry parameters influence forming quality [16]. As well, thickness and strength of the material impact formed part's quality. These characteristics of the sheet describe the forming force needed for the process. Due to the concentrated forming contact at a time, forming forces are drastically lower than drawing and molding methods – less energy is wasted. To decrease forming forces, materials can be heated by friction, radiation, and conduction [15]. However, experiments and research [15] revealed that the forming force is a complex parameter strongly linked with forming wall angle, depth of formed part, step size, contact friction, tool federate and geometry, and material characteristics. The geometry of forming tool and dimensions significantly influences forming forces and formability and is considered a critical factor in the process. There are three main types of tools that can be used are shown in Fig. 10. However, the tool's design can be chosen based on the requirements of an application.

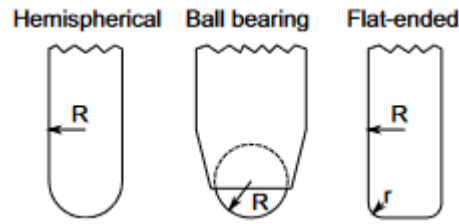


**Fig. 10.** Main types of SPIF tools.  $R$  – radius of the tool,  $r$  – radius of fillet [16]

Research revealed that a ball bearing tool has the potential to achieve better formability, surface quality, lower forming forces, and smaller shear compared to a rigid tool [15]. Another advantage of the ball bearing tool is that the ball can be easily replaced with a different diameter sphere if needed. Flat-ended and hemispherical tools require higher forming forces due to the more significant contacting area. Tools of the SPIF process can be made of different materials depending on the application. However, the tool's material slightly influences surface quality due to the friction between the blank and forming tool. Another influential parameter on formability is a toolpath. The toolpath of the processing can be planned and usually generated by CAD. There are a few main toolpath choices which are shown in Fig. 11.

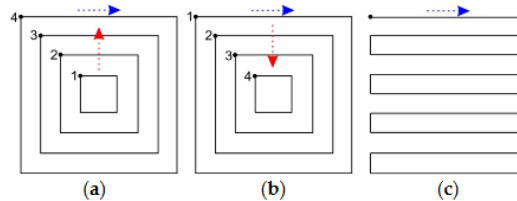


**Fig. 11.** Main toolpath strategies for ISPF process: a) parallel, upgrading, b) parallel, downgrading, c) zigzag, continuous [15]

Toolpath is chosen regarding on geometries of the needed part. A parallel toolpath is defined by step size between forming contours. This technique is commonly used due to its simplicity but has the disadvantage of leaving a force peak mark on every new layer. Zigzag or spiral toolpath is continuous with continuous descending of the tool. This technique does not leave any marks. However, multiple toolpaths can be used in one forming process to form a complex material.

Lubrication of contact points must be taken into consideration as well. Lubricant is an essential element in many forming processes; it reduces the tool's wear and distributes frictional temperature. It is an additional component to the process but can reduce forming forces and friction. Friction between the tool and the blank influences the surface quality and precision of the final product. Conducted experiment [17] revealed the positive influence of lubricants in incremental sheet forming. However, tests showed that lubricant is not a primary factor influencing the quality. The shape of the formed part and forming parameters such as step size, feed rate, and spindle speed influence formability. Literature analysis [16] showed that by decreasing step size, formability could be increased, by decreasing feed rate, formability can be increased, by increasing spindle speed, formability can be increased, too rotation direction has no influence on formability. Overall, SPIF is a complex process of stretching, bending, and tearing, and all the factors interact together simultaneously. The best outcome of the process can be achieved with a complex solution of all optimized characteristics. The process has an advantage in manufacturing costs, waste reduction, higher quality, and fast adaptation.

### 1.2.2. Two-point Incremental Forming

Similar to the robotic SPIF system is a two-point incremental forming (TPIF) process. These processes can be operated with CNC machines, purpose-built machines, robots, or hexapods with a tool attached with force, pressure, or temperature sensors. One possible two-point incremental forming method is with a partial or full die. As the name indicates, this technique requires a die and a moving blank holder. These requirements are the main drawback of the process due to the higher manufacturing costs compared to SPIF technology. The technology of TPIF is shown in Fig. 12.

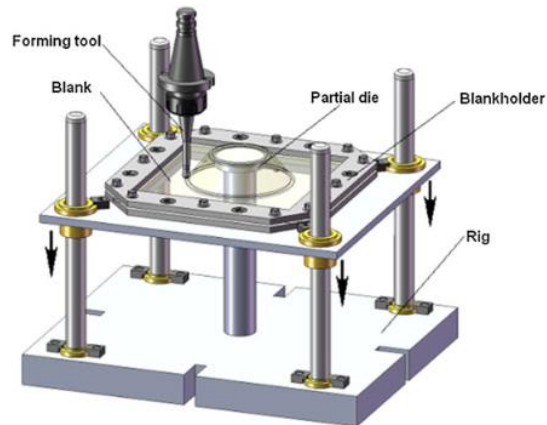


**Fig. 12.** Process of TPIF with a partial die [18]

Part is formed with a partial or full stationary die in this process. The sheet is clamped to the blank holder rigidly while the blank holder can move vertically. The forming tool moves along the blank holder by the program. Partial and full dies are used to ensure the support to the back of the sheet. This support reduces elastic recovery and improves accuracy through higher constraints of the blank, allowing wall thickness control [18]. However, the process is less flexible in rapid prototyping and small-batch production due to the dies. Since partial dies can be used for differently shaped parts, full dies are only intended for specific parts. Despite the differences, this technique is similar to the previous, and all influential quality parameters remain the same. The main advantage of this technology is higher geometry accuracy compared to SPIF [18].

A process where the additional tool is used instead of dies is called incremental forming with a counter tool or double-sided incremental forming (DSIF). The additional tool works in the same as the die – to support the back of the sheet for easier control of the process. The scheme of the forming technique is shown in Fig. 13.

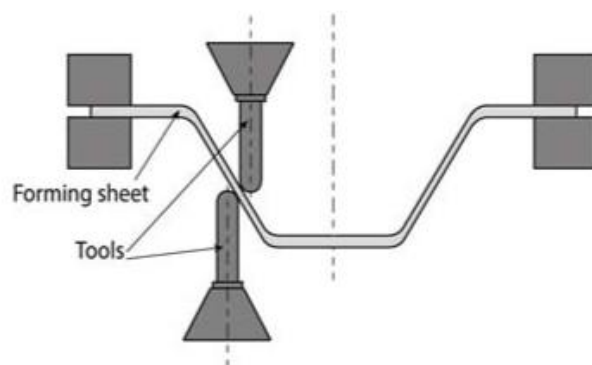


**Fig. 13.** Process of DSIF with a counter tool [19]

In this process, the sheet is clamped rigidly in the rig. The main forming tool positioned on the top of the blank, as in SPIF technology, is called master tool. This tool follows the programmed toolpath while another is programmed to follow the master tool and is called slave tool. The slave tool moves along the master tool at a distance of the thickness of the blank. There are two main strategies in DSIF that prevent the spring-back effect. These strategies are shown in Fig. 14. In the squeezing strategy, slave tool is squeezing the sheet to the master tool with force  $F_{bp}$ . The squeezing strategy allows the change of the stress and hydrostatic pressure values between two tools, increasing the formability of the blank. The reverse bending strategy contributes to the uniformization of the stress distributions.

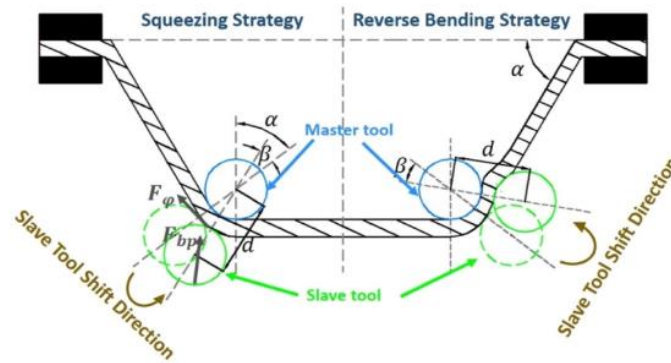


**Fig. 14.** The forming strategies of DSIF [15]

This process is more flexible than TPIF with a die but more complex because two robots must be programmed to execute the program. Compared to SPIF, DSIF has an advantage in forming speed, accuracy, rough surface quality, and higher forming angle [19]. Results of taken experiments [19] provide that the double-sided forming process has higher formability than single point incremental forming. Two tools allow to stabilize deformations and control the thickness of forming sheet, preventing spring backs. The additional tool also creates a compressive force which reduces shearing in the tool movement direction. However, controlling of thickness of the blank can lead to unpredicted contact loss between the tool and the polymer. Also, the energy consumption of the process is higher, and a bigger premise is needed to accommodate two machines in the production line.

### 1.3. ISPF Tools And Heating Possibilities

A tool and heating process play a tremendous role in the incremental sheet polymer forming. The quality and mechanical properties of the part depend on choosing the right tool and the critical temperature of processing. To apply the correct temperature in experiments, critical Glass transition temperature must be researched. Tool patients must be investigated to achieve the best processing quality and avoid errors. Main techniques must be revised to understand the most efficient polymer heating method.

#### 1.3.1. Glass Transition Temperature

The most crucial parameter in heating polymer processing is Glass transition temperature  $T_g$ . Applying this amount of heat increases mechanical properties and quality of part in post-process. Under the influence of this temperature, plastic changes its structure from solid to liquid or rubber.  $T_g$  temperature of every polymer depends on density, porosity, moisture, degree of crystallinity, the orientation of grades, size of molecules, and defects of the material [20]. In heating, at  $T_g$  temperature material's hardness and elasticity change drastically. As polymer reaches the rubbery state,

incremental sheet forming can be performed. Main polymers with their thermal properties are listed in Table 1.

**Table 1.** Polymers with their thermal properties [20]

Material	Crystalline melting temperature T <sub>m</sub> (°C)	Glass transition temperature T <sub>g</sub> (°C)	Crystallinity (%)
HDPE	136	-135	60
LDPE	103	-125	28
PP	163	-18	38
Nylon-6	223	47	30
PVDF	169	-35	49
PMMA	–	112	–
HIPS	–	93	–
PS	–	90	–
PC	–	145	–

One of the techniques to find thermal conductivity is the hot wire method. This technique allows measuring the thermal conductivity of polymers. The hot wire is an accurate and precise technology to identify the thermal characteristics of the material. According to ASTM D341 standard Glass transition temperature, crystalline melting temperature and crystallinity can be measured by differential scanning calorimeter with the heating rate of 10 °C/min. [20].

### 1.3.2. Polymer Heating Methods

Research of main polymer heating methods must be conducted to find the most eligible heating process for the experiment. Electromagnetic induction is one of the possible polymer heating methods. As polymers are non-conductive by their nature, additive materials are needed in this process to transform electromagnetic waves into heat. Usually, carbon fabrics or metallic woven are inserted into the sheet of polymers. The process is applicable when the ferromagnetic and conductive materials are placed in an electromagnetic field. Various applications of this method are researched. One of them is thermoplastic composite induction welding [21]. The process joins two polymers together while they are heated by electromagnetic induction. The technique can be automated and is classified into continuous and discontinuous welding. The continuous polymer welding robotic system is shown in Fig. 15.

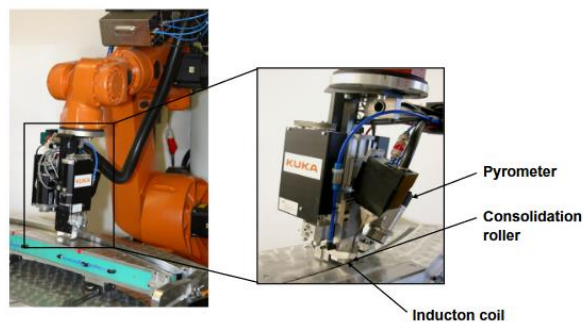


**Fig. 15.** Continuous polymer electromagnetic induction welding robot [21]

Other applications of polymer electromagnetic induction are thermoset curing, selective heating, triggering of processes in polymers while applying electromagnetic induction, and inductive mold heating. The application of thermoset curing allows quickly repairing damaged plastic by applying local heating. There is no need to remove a broken part in curing. Selective heating is a micro-scale process where the coil is heated on heatable material. This phenomenon is applicable in micro-welding due to the possibility of directing the heat into a micro-scale area. Triggering various effects in polymers is an essential process in shaping memory polymers. To trigger mechanisms that allow recovering the shape of the polymer part after a mechanical interaction, parameters such as temperature, light, and magnetic field must be changed [21]. Inductive mold heating is the system that heats the mold of polymers and ensures rapid and fluent control of the process. Tool's surface interfaces with a magnetic field and heat is produced. This technique allows producing shear edge parts. Unfortunately, there is too little research done to use the process widely.

Another polymer heating method is radiation heating. In the process, electromagnetic radiation is turned into heat. One of radiation heating possibilities, microwave heating, is similar to electromagnetic induction due to the requirement of additive materials. In the microwave heating process, microwave energy is turned into heat. Heat is delivered to the material through molecular interaction with an electromagnetic field. This technique has several advantages: improved mechanical properties of the part, energy and cost-saving, and efficiency due to the ability to heat polymer in the whole volume. [22]. However, heating efficiency depends on the dielectric properties of the polymer, and materials such as carbon fibers' layers are too reflective of radiation waves. Additionally, microwave heating has a nature of harmful radiation. Different radiation heating method is infrared light and laser. This process is based on electromagnetic energy conversion to the heat assisted by resonance vibrations. Since polymers tend to have many couplings, vibrations of 1,5  $\mu\text{m}$  frequency produce heating [23]. This heating application is flexible, easily controllable, and mainly used for welding polymers. However, the process is not widely used due to the lack of depth of waves penetration and absorption of heat in the surface layers.

Ultrasonic heating is a process where high-frequency mechanical vibrations are converted into heat. The technique is popular in thermoplastic welding due to the rapid progression, high quality, and possibility of automation. However, the ultrasonic heating process is inexpedient in heating volume as radiation heating is. Resistance heating is based on an electric current application on the polymer and application of the "Joule heating" effect [23]. This heating process applies to welding when materials are made out of composites. The convection and conduction heating process is a widely applicable and well-known method. The process is based on heat movement with gases and liquids. Hot gas, flame, oven, and hot shoe are primary convection and conduction techniques. In these processes, heat is carried by heated liquids and gasses to the surface of the polymer. However, the thermal conductivity of plastics plays a tremendous role in the efficiency of convection and conduction heating.

### **1.3.3. ISPF Tool Patents**

The technology of incremental sheet forming tools must be revised to acquire knowledge to design a self-heating forming tool. Proper equipment selection has a vast impact on part's quality and geometry. To acquire the most optimal design, patents of single point-forming tools must be reviewed.



Patent No. US 8,033,151 B2 [24] presents a tool that reduces forming forces by passing high-frequency ultrasonic sound waves. Ultrasonic incremental sheet forming is an energy and cost-efficient method. The frequency of waves in the process usually reaches 20 kHz [25]. Ultrasonic vibrations reduce friction between the tool and the sheet, improve the quality of the surface and precision quality. It allows the machine to create longitudinal ultrasonic vibrations, which work as a lubricant. The single point ultrasonic forming system mainly consists of a tool attached to the collector ring with a transducer. A simplified ultrasonic forming tool is shown in Fig. 16.

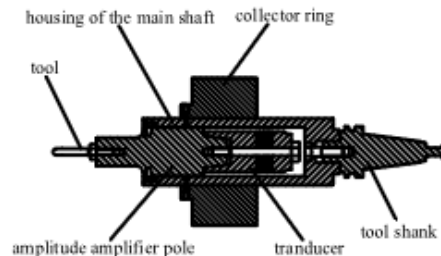


**Fig. 16.** Simplified structure diagram of ultrasonic incremental sheet polymer forming tool [25]

The equipment presented in the patent US 8,033,151 is similar to that described above but advanced in complexity. The apparatus has a platform that holds the sample, a motion control system, an ultrasonic generation system, thermal control system, and several sensors [24]. Ultrasonic waves generate energy directed to the sheet and cause vibration in the location. The isometric view of the patent's US 8,033,151 technology is shown in Fig. 17.

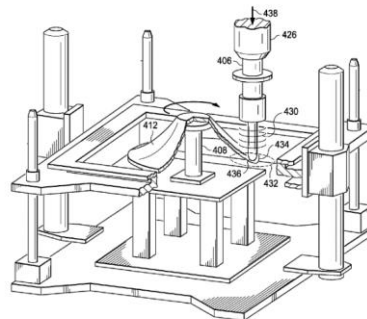


**Fig. 17.** Working principle of the patent's US 8,033,151 forming tool, 406, 426, 436 – stylus, 408 – forming tool, 412 – sheet part, 430 – ultrasonic energy, 432 – an area of energy impact, 434 – location of boundaries, 438 – applied forming force [24]

However, ultrasonic waves can cause machinery disruptions and defect the sheet's surface quality. If the process is used on metal sheets, high-frequency vibration can form cracks and wrinkles.

Another patent is registered in the US and presented as a robotic system of incremental sheet forming with local heating of the sample. Applied heat in the forming method reduces surface and precision errors and improves geometry and surface quality [26]. However, a tool diameter, a step size, forming forces, and a sheet thickness still play a huge role. As ultrasonic waves, local heating reduces friction between the tool and the part. Furthermore, increasing the temperature of the part can lead to better stainability of the material. Heating is applied to the minimal area needed for efficient forming. A



cooling system is installed in the patent to avoid unpredicted deformations due to thermal stress. The concept of patent US 7,984,635 B2 [27] is shown in Fig. 18.

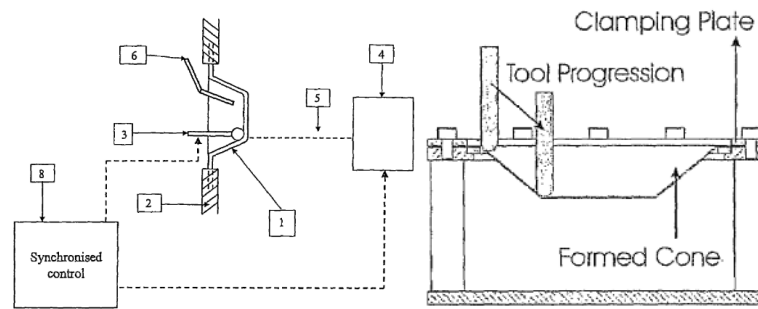


**Fig. 18.** Working principle of single-point tool forming patent US 7,984,635. 1 – sheet material, 2 – clamping system, 3 – forming tool, 4 – heating system, 5 – heat flux, 6 – cooling system, 8 – synchronization controller [27]

The system contains forming tool (3), which is moved by a 6-axis manipulator, a heating system (4) which locally heats the sheet (1), a cooling system (6) which ensures the quality of the part and synchronized control (8) which assures synchronization between heating and cooling systems. However, the solution increases forming machine construction complexity and reduces cost-effectiveness.

Overall, literature analysis revealed that vacuum bag forming, autoclave forming, close pressure thermoforming, 3D printing, and injection molding are perspective polymer forming processes. However, lack of flexibility, error occurrence, or insufficient quality prevent technologies from dominating polymer forming industry. An analysis proved robotic SPIF technology's superiority over discussed processes. Literature research revealed the most optimal heating method and theoretical temperature, material, tool, toolpath, and geometry influence the SPIF process. Analyzed patents of the tool gave the foundation for designing a novel self-heating tool. All gained knowledge is used in further research.

## 2. SPIF Self-heating Tool Design

Forming tool's feasibility is one of the essential parameters in the incremental sheet forming process. Conducted analysis of literature research revealed that the single point incremental forming is the most examined method among other technologies and has the potential to achieve high quality of production. Literature analysis of heating processes revealed an acceptable method of heating plastics – conduction heating method is used in further research. Gained knowledge about heating possibilities facilitates the solution of the tool. Analyzed patents prove the requirement of assistance of energy sources such as heat, ultrasonic or magnetic fields. One of the patents is close to the system required in this study and uses local heating assistance. However, the solution is too complex and can be redesigned and adopted to the needs. The concept of a single point incremental forming self-heating system is shown in Fig. 19.

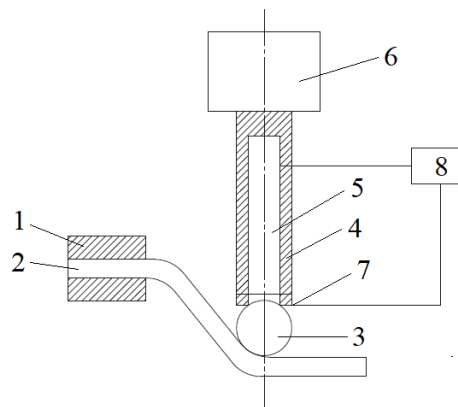


**Fig. 19.** The concept of SPIF self-heating tool: 1 – clamping, 2 – sheet, 3 – forming ball, 4 – tool, 5 – heating element, 6 – 6-axis robot hand, 7 – thermal sensor, 8 – heat control system

Components and heating effects must be researched and chosen correctly to design a proper self-heating tool to form polymer sheets. This chapter presents the main design stages of the self-heating tool and experiments needed to complete the research.

### 2.1. Heating Control System

Heating control system of the self-heating incremental forming tool is an essential part that ensures the temperature for the splendid incremental forming process. To design a proper heating control system, main components must be selected. One of them is a heating element. This essential component is responsible for heat generation to make the incremental forming process applicable. The temperature of PVC polymer must be high enough to reach the polymer's Glass transition temperature, which theoretically is around 55°C [20]. For the process, a 60 W soldering-iron heat element was chosen. Chosen heating element is shown in Fig. 20. This choice is justified by the requirement of small element to design a compact forming tool as much as possible. However, this type of heating element is presented for industry use. The first approach to investigate heating process is taken with a different 60W soldering-iron heat element.



**Fig. 20.** 60W soldering-iron heat element used in the investigation of incremental process

To automatically control and indicate the temperature of the self-heating tool, sensor and controller must be chosen. As the solution, REX-C100 48x48 AC 100-240V thermocouple RTD Input Digital PID Temperature Controller [28] and Thermocouple sensors K-type 0-800C [29] are chosen. They are shown in Fig. 21.



**Fig. 21.** Heating control system elements: REX-C100 48x48 AC 100-240V thermocouple RTD Input Digital PID Temperature Controller [28] (left). Thermocouple sensors K-type 0-800C [29] (right)

Digital PID Temperature Controller is a functional device that can control heater with an ON/OFF function to achieve a stable ambient temperature. It also allows regulating the intensity and cycling of heating. Proportional, integral, and derivative (PID) settings are adjustable in a menu of the device, operating temperature 0 – 400°C with a K-type thermocouple, accuracy 0,5%. A simple K-type thermocouple is chosen to use. Since the incremental forming process temperature is stable, 0,5 s responding time of this type of thermocouples should be enough to track temperature. The tool starts incremental forming with a heated tool already. The temperature drop when a polymer sheet is touched with the tool is not crucial since the tool is moving at high speed, and the sheet's area of the first touch should not be affected differently by a lowered temperature. The wiring scheme of a heating control system is shown in Fig. 22.

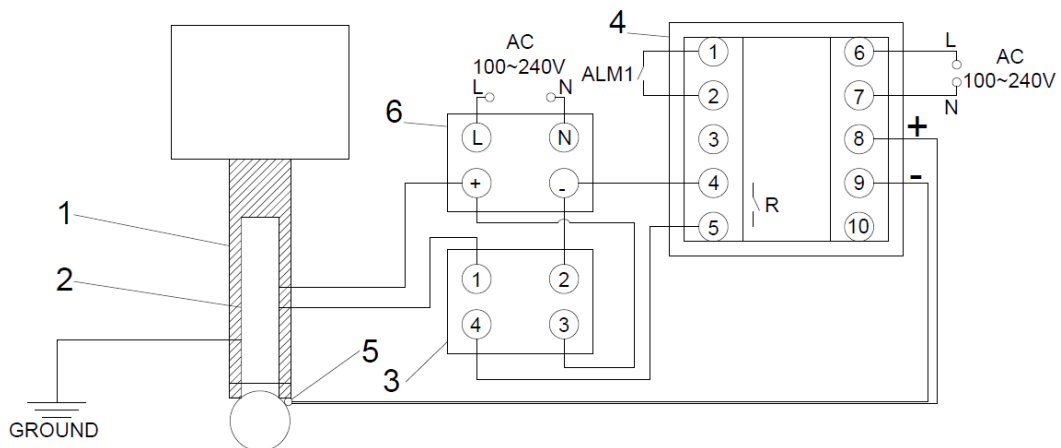


**Fig. 22.** Wiring scheme of a heating control system. 1 – Forming tool, 2 – 60W soldering-iron heat element, 3 – Solid-state relay (SSR), 4 – PID temperature controller, 5 – thermocouple, 6 – AC power supply

Heating element (2) attached to the tool (1) is wired through a solid-state relay (SSR) (3). This electric switch device turns on and off the heating element when an external AC power supply (6). When thermocouple (5) senses the required temperature, it sends information to the PID temperature controller (4). PID temperature controller connected through SSR turns off the heating element or changes voltage depending on the situation (depends on connection). To indicate temperature drops or rises, an alarm can be used. This solution is presented for industry exploitation. Further experiments are held without an automatic heat control system since temperatures in investigations are constant, and the overall formability of the new process is unexplored. Since this is the first approach, tool correction might be needed, and a control system can be implemented in the final design.

## 2.2. Heating Process Investigation

To use a 60 W soldering-iron heat element in the process, it is essential to know heating element and PVC polymer heating possibilities. Since further experiments will be held without a controlling system, it is necessary to find the heater's temperature dependency on the supply's power and heat distribution in the polymer sheet. These experiments will define the boundaries of inputs and variables for further research. An investigation of the heating element's capabilities was held at room temperature and repeated three times with each temperature to increase the accuracy of the outcome. The scheme of the held experiment is shown in Fig. 23 (left) and the set-up view in Fig. 23 (right).

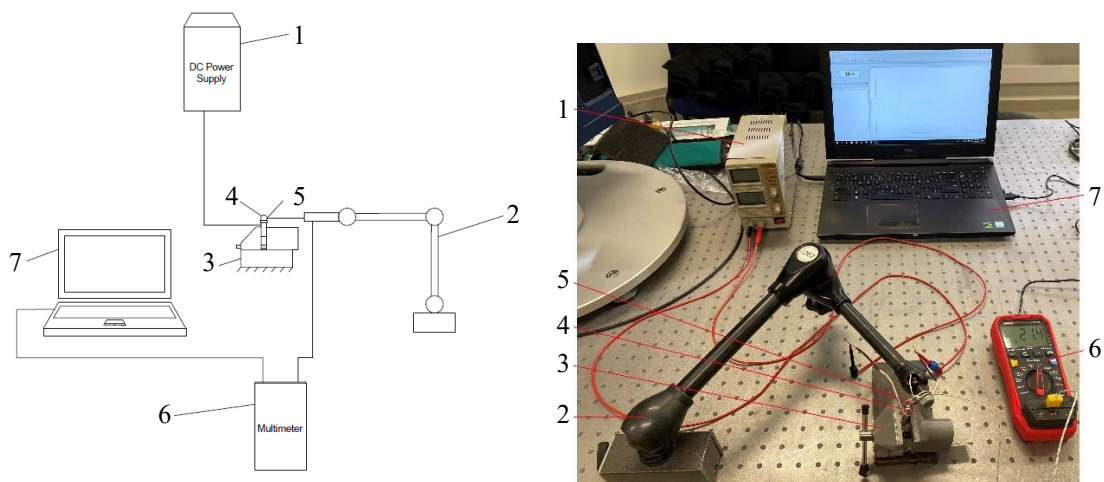


**Fig. 23.** The experimental calibration scheme (left) and set-up view (right). 1 – DC Power Supply HY1803D (0-18V, 3A), 2 – Stand, 3 – Clamp, 4 – Heater with magnet and ball, 5 – Thermocouple, 6 – Digital Multimeter UNI-T UT161D, 7 – PC

The research was performed by changing the current of the DC Power Supply HY1803D (1) and measuring the temperature on the forming ball's (4) furthest point from the heating source. The ball was attached to the heater with a magnet. Since the heater has steel parts, magnetism ensures the rigidity of the construction while investigating. The temperature of the forming sphere (4) was indicated with a thermocouple (5) stationary attached to the stand (2). A heater is fixed in the clamp (3). Thermocouple (5) sends information to the multimeter UNI-T UT161D (6) and the PC (7). To prevent heat losses and inaccurate results due to the conduction, textolite STAF-1 plates were used in the contact regions of the heating element and clamps. Textolite STAF-1 is characterized by high flame resistance and low thermal conductivity [29]. A closer view of the experimental setup is shown in Fig. 24.

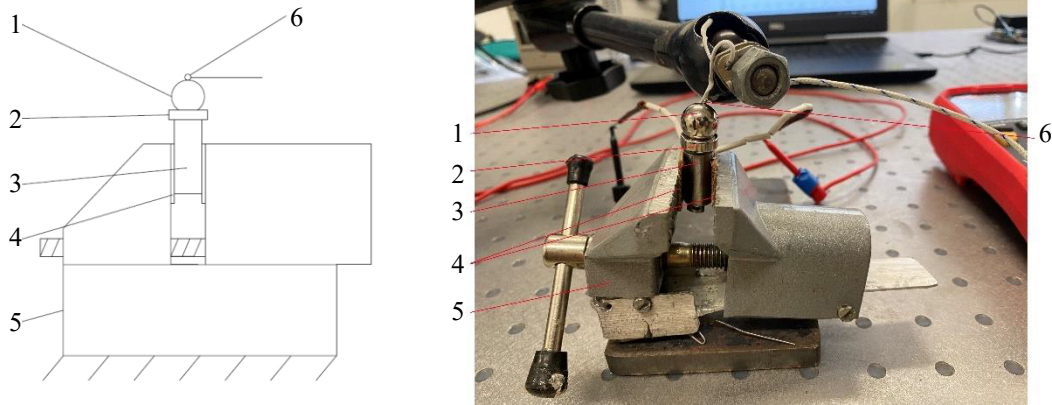


**Fig. 24.** Scheme of heater construction of carried research (left) and setup view (right). 1 – ball, 2 – magnet, 3 – heating element, 60W 4 – textolite STAF-1 plates, 5 – clamping, 6 – thermocouple

Experiment was held with  $\varnothing 12,5$  mm forming ball and four different powers: 0,3W, 0,09A, 0,12A and 0,18A. The results of the investigation are shown in Fig. 25. Results of the experiment revealed that different temperatures are reached with different supplied power: at 0,3W heater reaches a peak of 26,1°C, at 0,675W – 33,1°C, at 1,2W – 47,7°C, and 2,7W – 75,3°C. Also, it was noticed that the forming ball's temperature settles down over different time frames: 26,1°C in ~600s (10min), 33,1°C in ~900s (15min), 47,7°C in ~1500s (25min), and 75,3°C in ~1800s, (30min) These observations prove that a temperature control system is required for production usage due to inertia of the heating element and temperature sensitivity to DC power change. However, results approved that the heating element can reach temperatures needed for the incremental sheet forming process and provided power–temperature dependency, which can be used to identify when the temperature is settled.

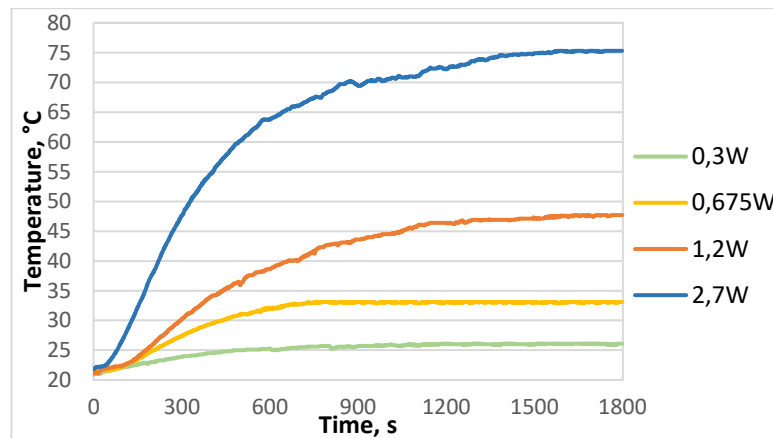


**Fig. 25.** Temperature values of  $\varnothing 12,5$  mm sphere under different power versus time

During the investigation, moving the thermocouple on the forming sphere provided information that the ball's temperature differs in its volume. The sphere temperature near the magnet is higher than the temperature at the forming point by 1°C. Stainless steel's thermal conductivity is conditionally high – 15W/(mK) [30]. However, the volume of the sphere heats unequally. It is an important nuance that must be considered in further research since the ball was not rotating in this experiment. The temperature of a rolling ball can differ from the measured stationary ball's temperature.

Another conducted thermal experiment allowed us to evaluate thermal losses in the polymer material, ensure the heater's feasibility and approach forming temperature of the sphere. One of the aims of this approach was to find polymer sheet temperature in contact with the ball at different temperatures.



Another one is finding the forming sphere's temperature, which reaches Tg temperature in plastic. The experiment was held at room temperature and repeated three times with every temperature to increase the accuracy of the results. The scheme of the held experiment is shown in Fig. 26 (left) and the set-up view in Fig. 26 (right).

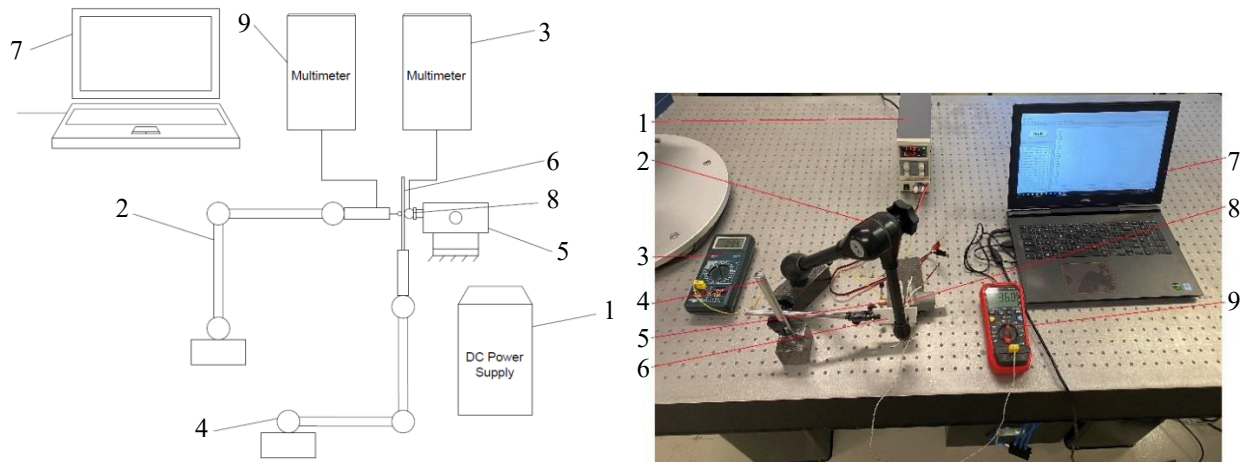


**Fig. 26.** Scheme of polymer's heating investigation (left) and setup view (right). 1 – DC Power Supply HY1803D (0-18V, 3A), 2, 4 – Stands, 3 – Digital Multimeter CHY 24CS LCR METER, 4 – Heater with magnet and ball, 5 – Clamp, 6 – Sample, 7 – PC, 8 – Heating element, 9 – Digital Multimeter UNI-T UT161D

During this experiment, a 3mm thickness polymer sheet (6) with drilled 0,5mm, 1mm, 1,5mm, 2mm, and 2.5mm depth and 2 mm diameter holes were heated. The sample was attached to stand (4) to reduce displacements and loss of contact. As in the previous investigation, a forming ball with the heater (8) was clamped with textolite STAF-1 plates. Two multimeters were used in this experiment: digital multimeter UNI-T UT161D (9), which indicated the temperature of the polymer sample on the other side of the heating surface, and another digital multimeter CHY 24CS LCR (3) was used to track the temperature of the forming ball. Thermocouple of the first multimeter was attached to stand (2) and placed in drilled holes. Heating was generated with DC Power Supply HY1803D (1), and data from digital multimeter UNI-T UT161D was sent to the PC (7). A closer view of the experimental setup is shown in Fig. 27.

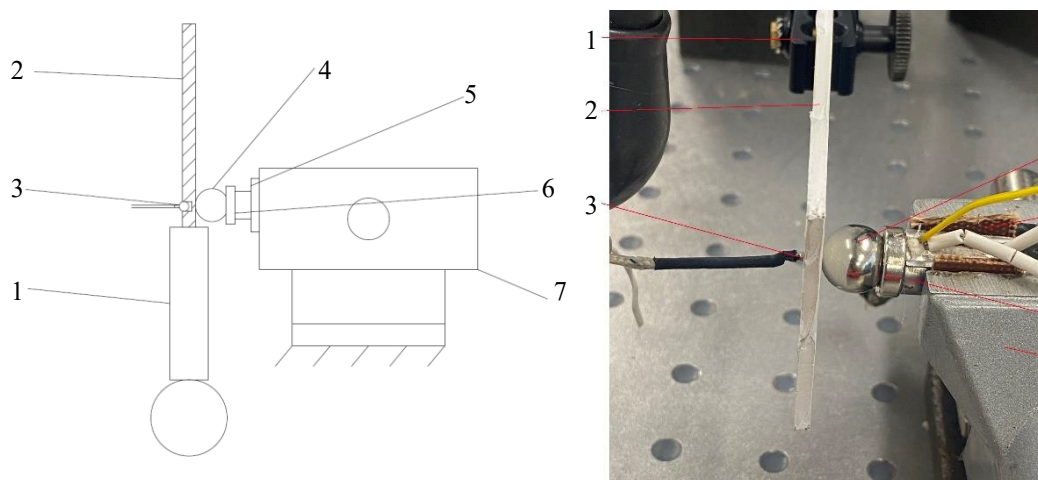


**Fig. 27.** A view of held investigation's schematic (left) and experimental setup (right). 1 – Stand, 2 – Sample, 3 – Thermocouple, 4 – Forming ball, 5 – Textolite STAF-1 plates, 6 – Heating element, 7 – Clamp

An experiment was held with a  $\varnothing 12,5$  mm forming ball and four different sphere temperatures: 50°C, 60°C, 75°C, and 100°C. When a forming ball (4) reached investigation temperature, sample (2) with a thermocouple at room temperature (3) were touched to the sphere. Temperatures of different layers of material at different ball temperatures were indicated. The temperature versus time of the polymer heating process was also tracked. Only one temperature – 75°C of the forming sphere was analyzed from a time perspective since this amount of heat triggers Tg temperature in PVC plastics. Results of the investigation are shown in Fig. 28. and Fig. 29.

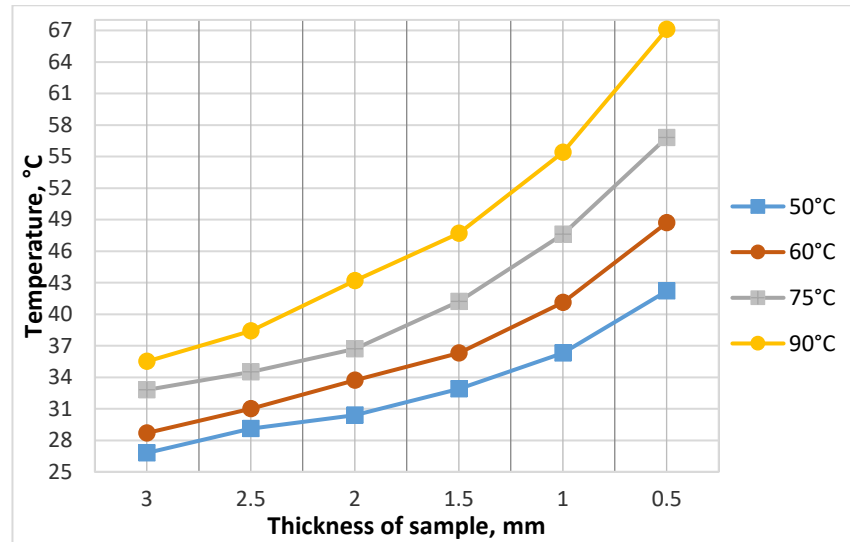


**Fig. 28.** Temperature values of sheet layers under different forming ball temperatures versus thickness of a sheet

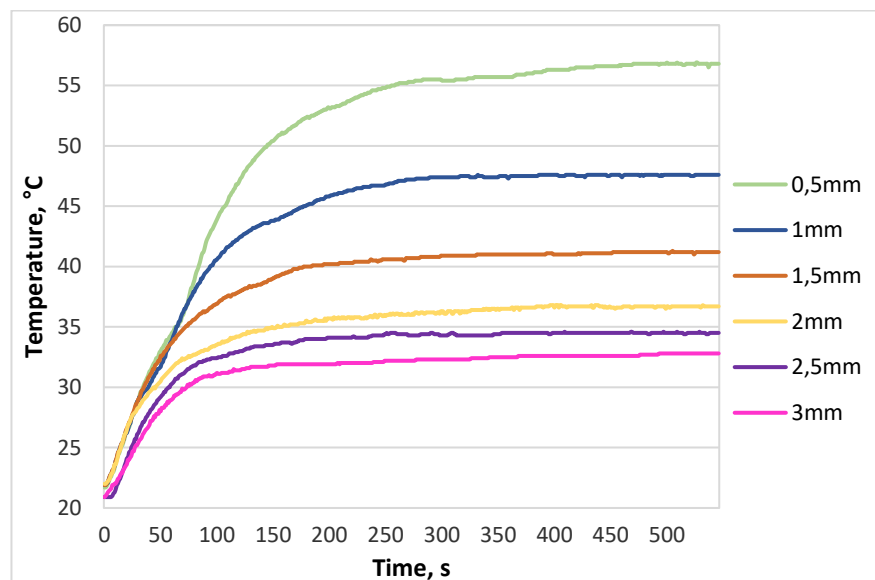


**Fig. 29.** Temperature values of sheet layers under 75°C forming ball temperature versus time

The results of carried experiments revealed that under 75°C sphere's temperature, polymer temperature in 0,5 mm thickness reached 56,8°C, and this temperature can be considered theoretical forming temperature to achieve the best results. However, 32% of generated heat at the 75°C temperature of forming ball was lost in the conduction process. Results showed that the temperature difference in 0,5 mm thickness and 3 mm thickness material is more than 20°C. The experiment revealed that deeper layers of material reach their highest temperature faster than closer layers to the

heating element. An exponentially higher temperature of forming ball is needed to heat deeper layers. The investigation provided valuable information that it takes about 8 minutes of heating with a 75°C ball to reach optimal forming temperature in 0,5 thickness of the material.

### 2.3. Design of SPIF Self-heating Tool

Selected heating element, temperature controller, and thermophore allow designing a SPIF self-heating tool. Literature analysis presented three main forming tool types, and one of them is the ball bearing tool. This structure is selected for the investigation. Since the tool is not rotating, the ball is allowed to rotate freely to reduce friction. The heating element is inserted into the tool. However, the heating element can not contact the steel tool directly due to the high thermal conductivity of the steel. Loss of the heat would lead to higher power consumption Heater is fixed in the tool with low thermal conductivity bushings. Bushings are made of textolite rods to reduce temperature loss in the tool. A designed novel self-heating tool is shown in Fig. 30. Heating element (1) is inserted into the tool (4). To avoid energy losses, an element is isolated from the steel with textolite bushings (5, 6). Bushings also position and tighten the heating element in the tool. Contacts of the heater are brought out through the gap of the tool. The magnet ring (2) is used to ensure the position of the forming ball (3). The tool's drawings and technical data are provided in Appendixes 1 – 5.

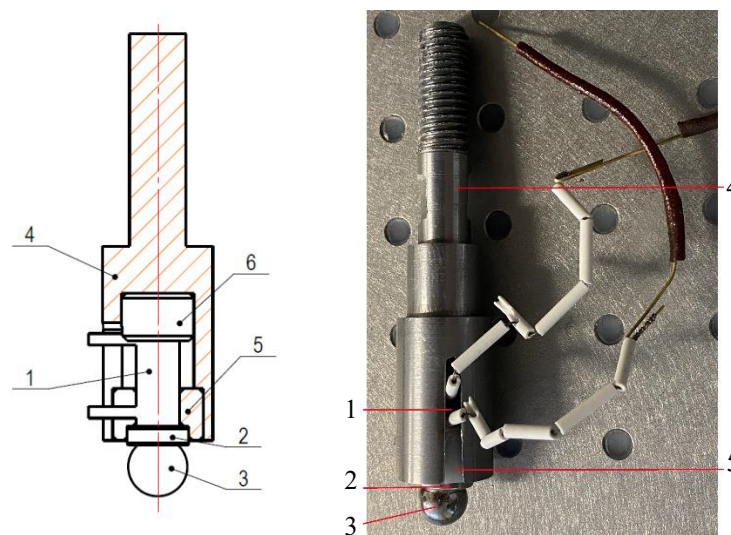


**Fig. 30.** Designed SPIF self-heating tool. 1 – Heating element, 2 – magnet, 3 – forming ball, 4 – tool, 5, 6 – bushings

Overall, self-heating forming tool for incremental single point forming was designed. The tool consists of a steel tool shell, 60 W heating element, magnet, forming ball, and textolite bushings which forbid heat transferring loss to the steel. An automatic control system is presented to implement a self-heating tool in manufacturing: a PID temperature controller with an SSR and thermophore to indicate temperature. Investigation with a heating element revealed the dependency between the DC supply's power and heater temperatures. Results showed that the forming ball's temperature used in further research (75°C) was reached with 2,7 W power, and it took about 30 min. The results of carried experiments revealed that under 75°C sphere's temperature, polymer temperature in 0,5 mm thickness reached 56,8°C, and this temperature can be considered theoretical forming temperature to achieve the best results. An exponentially higher temperature of forming ball is needed to heat deeper layers. The investigation provided valuable information that it takes about 8 minutes of heating with a 75°C ball to reach optimal forming temperature in 0,5 thickness of the material.



### 3. Experimental Research of Self-heating Forming Tool

The self-heating incremental process feasibility and efficiency can only be acquired through experimental research. Various experiments must be held to use a novel self-heating incremental forming tool in the production. Before using the tool in forming a blank, main parameters such as the temperature of the forming sphere and forming forces must be analyzed. Static and dynamic experiments must be conducted since the heat amount transferred to the forming sphere is different from the previous research. The static approach reveals the novel tool's formability dependency on forming forces and temperature. A dynamic approach provides valuable information about polymer formability and process temperature boundaries in the dynamics. Obtained data is used in further simulating and experimental research to achieve the best quality of incremental sheet forming.

#### 3.1. Static Experiment of a Self-heating Forming Tool

A static experiment approach of self-heating incremental forming tool can lead to a better understanding of temperature and forces contribution to the process quality. Studying static tool heating to the polymer sheet can reveal losses and distribution of heat and provide valuable information about surface quality. A study allows identifying the depth of the imprint of the forming tool's sphere at different temperatures and forces. An experiment was held at room temperature and repeated three times to increase the accuracy of the outcome. As a result, average values are presented in the results. Two different spheres were used to understand the impact of forming pressure on the blank:  $\varnothing 12,5$  mm and  $\varnothing 11$  mm. The research was held with three different temperatures and three different forming forces. Other investigations [32] revealed that longitudinal incremental forming force in the polymers does not exceed 400N under local whole sheet heating, therefore, the maximum values of 100N, 200N, and 300N force are used in this experiment – the whole bottom of the blank is touching the surface of the stand – the values of stresses in the sheet are higher than in the process of incremental forming. No spring back is allowed. Experiment temperatures were chosen according to the Glass transition temperature equal to  $55^{\circ}\text{C}$  in PVC plastics. However, value can vary depending on the composition of the material. Previous research revealed that a  $75^{\circ}\text{C}$  temperature forming ball is required to reach  $55^{\circ}\text{C}$  temperature in a polymer. To find formability dependency on the temperature,  $50^{\circ}\text{C}$ ,  $75^{\circ}\text{C}$ , and  $100^{\circ}\text{C}$  temperatures are analyzed. The schematic view of a held experiment is shown in Fig. 31 (left) and the set-up view in Fig. 31 (right).

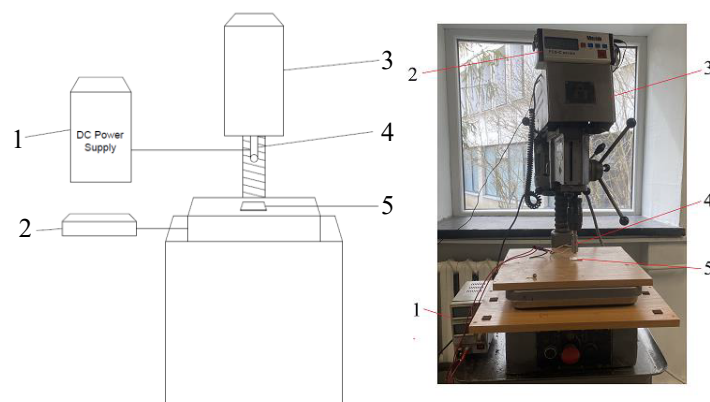


**Fig. 31.** Schematic view of static self-heating forming tool experiment (left), setup view (right). 1. – DC Power Supply HY1803D (Mastech Digital, Inc., USA), 2 – FCS-C series platform scales (UAB Mingeda, Lithuania), 3 – Praktika drilling machine TU2-024-2546-70, 4 – Designed SPIF self-heating tool, 5 – PVC ESA-D 3mm thickness polymer sheet

During the experimental research, the forming tool (4) was heated by increasing the power of the heating element by changing the current and voltage of DC Power Supply HY1803D (1). PVC ESA-D 3mm thickness samples (5) aligned on the FCS-C platform scales (2). Forming tool was attached to the drilling machine Praktika TU2-024-2546-70 (3). With each temperature, samples were affected by different forces. To track the temperature of the tool's sphere, multimeter UNI-T UT161D with a thermocouple was used. When the temperature of the contacting point of the sphere reaches and stays at the experimental temperature, the machine heats the polymer and stamps samples with the self-heating tool for 60 s with each specified constant force. Samples after the experiment are shown in Fig. 32.

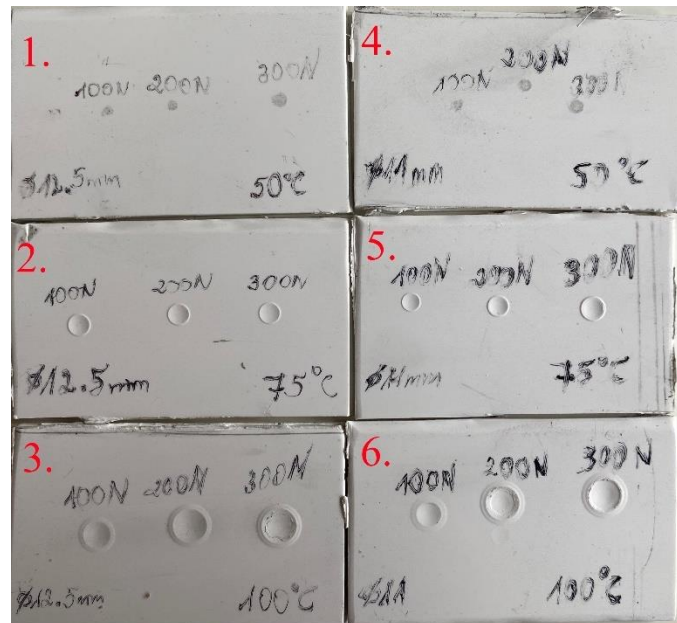


**Fig. 32.** Samples after the static experimental research: 1. – Sphere Ø12,5mm, 50°C, 2. – Sphere Ø12,5mm, 75°C, 3 – Sphere Ø12,5mm, 100°C, 4. – Sphere Ø11mm, 50°C, 5. – Sphere Ø11mm, 75°C, 6. – Sphere Ø11mm, 100°C

When the sample is affected by the machine, the mass of the pressing is shown in the platform scales. Mass of shown weight multiplied by standard gravity is equal to applied forces. Since the polymer is a plastic material, deformations can be noticed due to the force and heat – the value in the platform scales drops in time. The higher temperature and forces, the more significant decrease in the scales, and deeper prints are noticed in the samples. The principle of the process with variables is shown in Fig. 33.

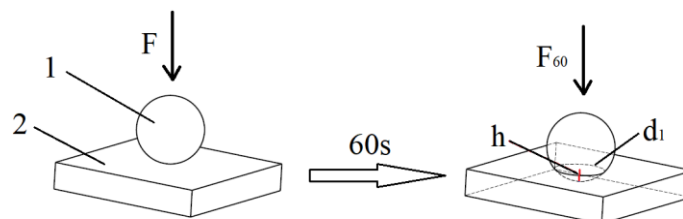


**Fig. 33.** The principle of the static experiment: 1 – hot sphere, 2 – sample,  $F$  – initial force,  $F_{60}$  – reduced force after 60 seconds of deformation,  $h$  – depth of the imprint,  $d_1$  – diameter of the imprint

It is essential to identify the depth of the imprint and difference in forces to evaluate the surface's quality and correctly describe the forming process itself. The depth of the imprint is an important parameter and is bounded by the incremental forming step size ( $\Delta z$ ). Step size is the depth of the tool's downgrading each iteration of forming cycle. Choosing step size incorrectly can lead to defects such as wrinkles, cracks, and twisting. Similar experiments on step size impact on forming quality proved that  $\Delta z$  is a variable, dependent on different thickness of the sheet, forming speed, temperature, and angle of forming [33]. Various outcomes at different step sizes of the forming process are shown in Fig. 34.

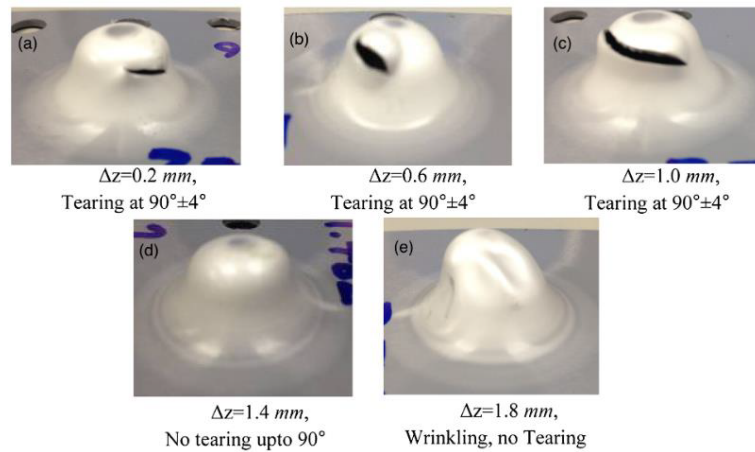


**Fig. 34.** Incremental sheet forming quality dependence on step size. The thickness of the sheet – 12mm [33]

Depths of imprints of the static experimental research are found by using high accuracy laser displacement sensor. Laser displacement sensor precisely measures displacements that are distant from the sensor 8 cm – samples are placed at this distance from the sensor. The process of measuring is shown in Fig. 35. Measurements were repeated three times, and average values were listed in the results.

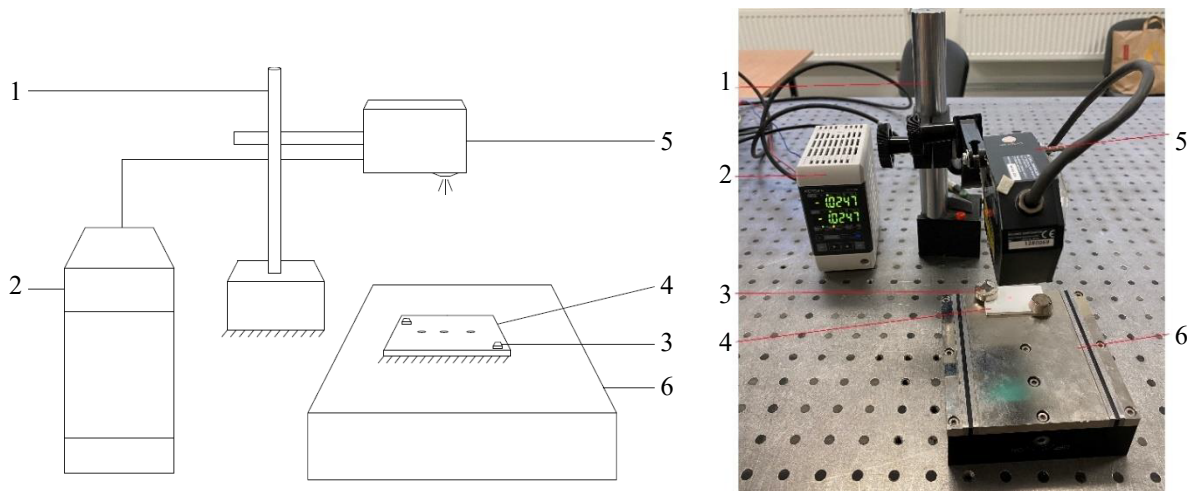


**Fig. 35.** Set-up schematic view of static experiment result measurements (left), set-up view (right). 1 – Stand, 2 – Keyence Display panel (Keyence, Inc., USA), 3 – Magnets, 4 – Sample, 5 – High speed, high accuracy CCD Laser Displacement Sensor (Keyence, Inc., USA)

The process of measurements includes measuring four points around the imprint and, finding the average distance between the surface and the sensor, measuring the deepest imprint point. Average distance values are subtracted from the values of imprint. Samples of the static experiment (4) are

clamped with magnets (3) to the moving table (6). The table must be leveled with a level since a sidelong surface can lead to inaccuracies in measurements. The table was carried under the laser beam of high accuracy CCD Laser Displacement Sensor LK-G82 (5). The sensor was rigidly attached to the stand (1). Values of the indicator were shown in Display panel LK-GD500 (2). Variables and results of the experiment are listed in Table 2.

**Table 2.** Results of the static experiment with a self-heating forming tool

	Sphere with Ø12,5 mm						Sphere with Ø11 mm											
	50°C			75°C			100°C			50°C			75°C			100°C		
Applied force F, N	100	200	300	100	200	300	100	200	300	100	200	300	100	200	300	100	200	300
Force after 60 s of impact F <sub>60</sub> , N	94	174	239	89	169	247,5	53,5	137	205,5	93	169	230	90	165	228,5	35	108	152
The difference ΔF, N	6	26	61	11	31	52,5	46,5	63	94,5	7	31	70	10	35	71,5	65	92	148
The depth of imprint h, mm	0,0033	0,0071	0,0143	0,0604	0,0777	0,0984	0,1148	0,1764	0,2359	0,0098	0,0209	0,0349	0,0816	0,0986	0,1301	0,1385	0,218	0,2989

Experimental research revealed that temperature, the force of press, and the sphere's diameter significantly influence the process. An accomplished experiment revealed that the sphere's diameter influences the depth of the imprint. Imprints' depth dependency on forming sphere diameter and temperatures are shown in Fig. 36.

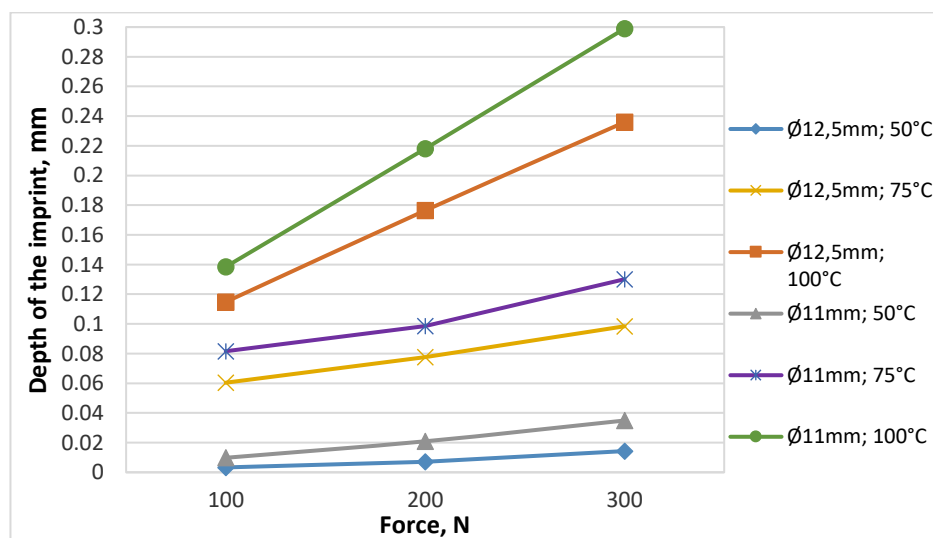


**Fig. 36.** Depth of imprint values under different forming ball diameters and temperatures versus applied forces

The dependency graph revealed that the depth of the imprint is directly proportional to applied force under the same size forming ball. However, the perpendicularity of the line depends on the sphere's temperature. Forming with a smaller sphere creates a slightly deeper imprint than the bigger one. This phenomenon can be explained as a force applied perpendicular to the surface per unit area. The smaller diameter of the forming tool's sphere, the deeper imprint is achieved with a greater force. This observation can conclude that a smaller diameter sphere requires lower forming forces to achieve the same imprint depth as with a bigger diameter. However, visual analysis of samples showed that higher surface quality could be achieved with a bigger diameter sphere under the same conditions. This property can be seen at higher temperatures of spheres. Since pressure is higher in the forming process with a smaller sphere, sharper and bigger melt rings are noticed in samples at higher temperatures. This statement concludes that a bigger forming sphere can achieve better surface quality. Results of the experiment revealed that the system's temperature has a significant influence on polymer formability. Increasing temperature from 50°C to 75°C increased formability 3,72 times, and increasing temperature from 75°C to 100°C increased formability 2,3 times. Experimenting with close temperature to PVC Tg temperature revealed best results. The imprint's depth under 75°C and 300 N equals 0,0984 mm and has no defects. A test at 100°C revealed that at this temperature, plastic is melting, the surface of the imprint is rough and porous. Samples tended to stick to the hot forming ball. This temperature is too high to use in the static processing of PVC polymer. However, an experiment was held with a preheat and 60 seconds of steel sphere and plastic contact. In the dynamic incremental sheet forming process, the tool moves, and the material cannot embezzle the same amount of heat as in the static state. Overall, the static investigation provided valuable data to obtain a temperature and forced dependency on formability and revealed the influence of forming sphere size on the quality. The experimental data will be used in the further investigation and simulation of the case.

### **3.2. Dynamic Experiment of a Self-heating Forming Tool**

A dynamic experiment with a self-heating forming tool is a closer approach to the incremental sheet forming process. However, in this experiment, as in the static, the whole bottom of the sample is touching the stand's surface. Therefore, the tool makes a groove instead of performing an incremental step. Studying the movement of the tool on the surface can reveal the material's formability in dynamics at different temperatures and forces and provide valuable information about the surface quality. An experiment was held at room temperature and repeated three times to increase the accuracy of the outcome. As before, two different spheres were used to understand the impact of forming pressure on the blank: Ø12,5 mm and Ø11 mm. The research was held at four different temperatures. To investigate plastic under critical conditions, higher experimental temperatures are chosen. The amount of heat transferred to the polymer area depends on tool movement speed in this approach. To find the boundaries of heating that could be used in the incremental forming process, 50°C, 75°C, 100°C, and 120°C temperatures were analyzed. To find eligible force boundaries, 100N, 200N, 300N, 400N, and 500N forces were determined. The schematic view of a held experiment is shown in Fig. 37 (left) and the set-up view in Fig. 37 (right).



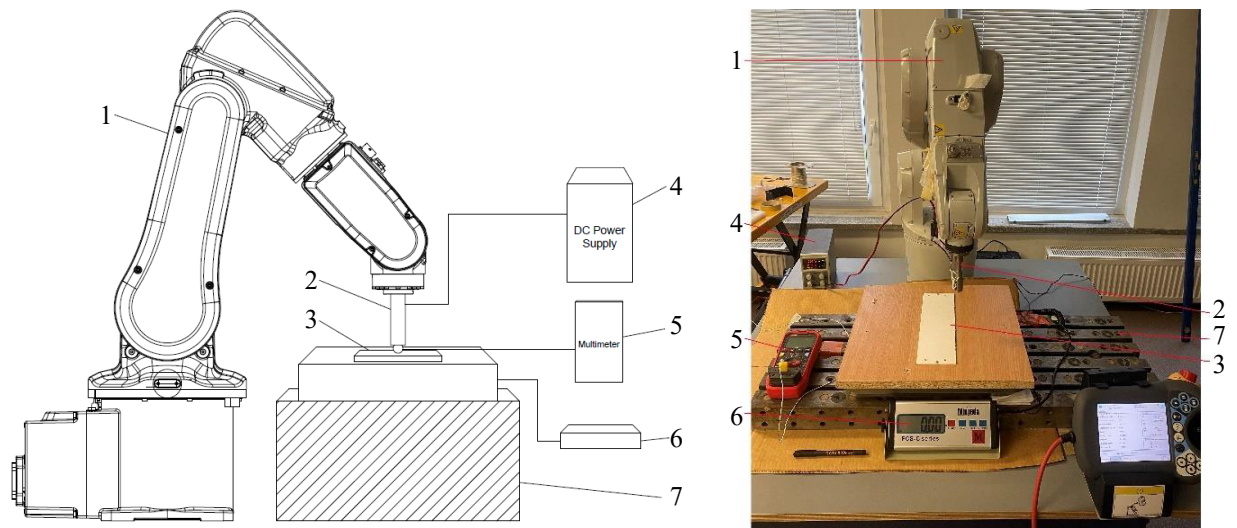


**Fig. 37.** Set-up schematic view for dynamic self-heating forming tool experiment (left), set-up view (right). 1. – Manipulator ABB IRB1200 (ABB Robotics & Discrete Automation, Västerås, Sweden), 2 – Designed SPIF self-heating tool, 3 – PVC ESA-D 3mm thickness polymer sheet, 4 – DC Power Supply HY1803D (Mastech Digital, Inc., USA), 5 – Digital Multimeter (Uni-Trend Technology Co., Ltd., China), 6 – FCS-C series platform scales (UAB Mingeda, Lithuania), 7 – Holding frame

As well as before, during the experimental research, the forming tool (2) was heated by increasing the power of the heating element by changing the current and voltage of DC Power Supply HY1803D (4). PVC ESA-D 3mm thickness sample (3) clamped on the FCS-C platform scales (6). During the experiment, it was essential to maintain a horizontal blank level. Wrongly set samples could increase or decrease forces and geometry inaccuracy of imprinted path. A level was used to determine the horizontal position of the blank. Samples with scales were clamped to the holding frame (7). Forming tool was attached to the ABB IRB1200 manipulator (1). With each temperature, samples were formed with a constant 6,33 mm/s speed and affected by 100N, 200N, 300N, 400N, and 500N forces. Since the tool is moving and the amount of heat transferred to one unit of polymer volume is lower than in the static experiment, the assumption was made that more immense forces must be analyzed to maintain similar depth imprints as in the previous approach. To track the temperature of the tool's sphere, multimeter UNI-T UT161D (5) with a thermocouple was used. When the temperature of the contacting point of the sphere reaches and stays at the experimental temperature, the manipulator is operated to form a groove on the blank. Samples after the experiment are shown in Fig. 38. When the tool interfaces with the sheet weight of pressing are shown in the platform scales. As in the previous experiment, mass multiplied by standard gravity equals applied forces. As in the static investigation, when the tool touches the sheet's surface, heat softens the blank, and deformations appear – the weight shown in the scales starts to drop. When the tool starts to move, forces start to grow again because one unit of material's volume gets less heat, and the material's hardness is higher than starting point's hardness. The higher temperatures and forces, the deeper groove can be noticed. The principle of the process with main variables is shown in Fig. 39.



**Fig. 38.** Samples after the dynamic investigation

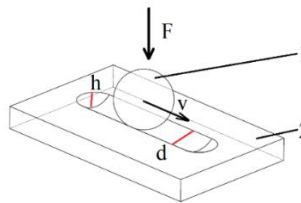


**Fig. 39.** The principle of the dynamic experiment: 1 – hot sphere, 2 – sample,  $F$  – initial force,  $h$  – speed of moving sphere,  $h$  – depth of the groove,  $d$  – width of the groove

The procedure of results measuring is precise as in the previous experiment. As in the static investigation, the depth of grooves was found by using high accuracy laser displacement sensor. Measurements were conducted three times, and average values were calculated. The process of measuring is shown in Fig. 40.

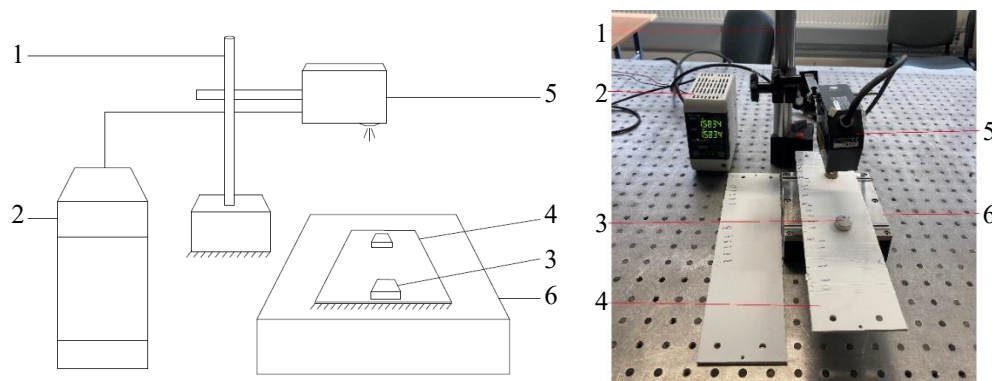


**Fig. 40.** Set-up schematic view of dynamic experiment result measurements (left), set-up view (right). 1 – Stand, 2 – Keyence Display panel (Keyence, Inc., USA), 3 – Magnets, 4 – Sample, 5 – High speed, high accuracy CCD Laser Displacement Sensor (Keyence, Inc., USA)

The process of measurements includes measuring two points (above and below the groove) average distance of the surface to the laser sensor, measuring the deepest groove point, and average distance values subtracting from the values of grooves. Samples of the dynamic experiment (4) were clamped with magnets (3) to the moving leveled table (6). The table was moved under the laser beam of high

accuracy CCD Laser Displacement Sensor LK-G82 (5). The sensor was rigidly attached to the stand (1). Values of the indicator were shown in Display panel LK-GD500 (2). The results of the experiment are listed in Table 3.

**Table 3.** Results of the dynamic experiment with a self-heating forming tool

Sphere with $\varnothing 11$ mm																				
	50°C					75°C					100°C					120°C				
Force F, N	100	200	300	400	500	100	200	300	400	500	100	200	300	400	500	100	200	300	400	500
Depth, h, mm	0,0019	0,0024	0,0033	0,0049	0,0068	0,0025	0,0046	0,0087	0,0131	0,0197	0,0083	0,0131	0,019	0,0254	0,0311	0,0194	0,0364	0,0661	0,0925	0,1352
Sphere with $\varnothing 12,5$ mm																				
	50°C					75°C					100°C					120°C				
Force F, N	100	200	300	400	500	100	200	300	400	500	100	200	300	400	500	100	200	300	400	500
Depth, h, mm	-	-	-	-	-	0,002	0,0038	0,0066	0,0091	0,015	0,0069	0,0113	0,0169	0,0212	0,0275	-	-	-	-	-

Dynamic experimental research proved legitimate of static investigation results that temperature, forming force of press, and sphere diameter influences the forming process. Nevertheless, the dynamic experiment revealed that grooves are more trivial than static imprints even under greater forces and higher temperatures. This observation leads to the statement that the temperature and forces of the forming tool should be changed depending on the movement speed of the tool. Grooves' depth dependency on forming sphere diameter and temperatures are shown in Fig. 41.

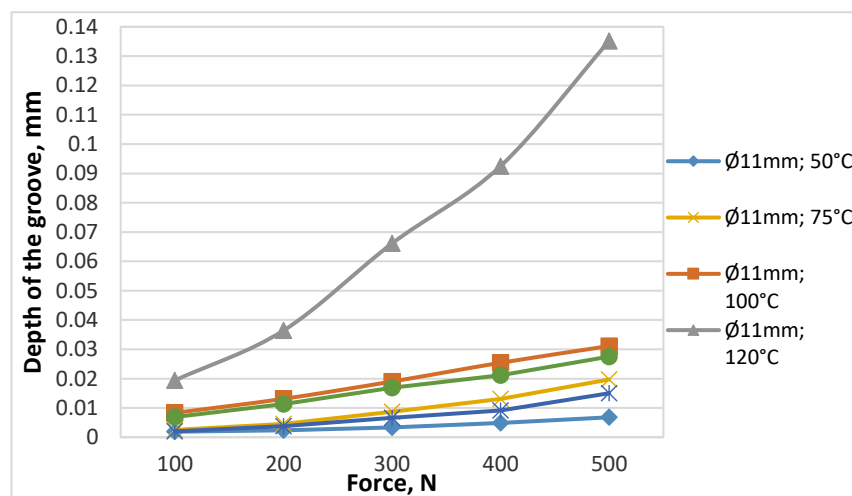


**Fig. 41.** Depth of groove values under different forming ball diameters and temperatures versus applied forces



Results revealed that the depth of the groove is directly proportional to applied force under the same size forming ball. However, the perpendicularity of the line depends on the sphere's temperature. It was noticed that a smaller sphere forms a deeper groove under the same conditions. However, the Ø12,5 mm sphere formed a smoother path under exact experimental conditions compared to the Ø11 mm ball. The 50°C and Ø11 mm sphere experiments proved that this temperature is too low to perform a valid dynamic process. Grooves are indistinct with all experimental forces and cannot be noticed by an eye or touch. Due to inexpedient results, it was decided not to repeat the 50°C experiment with a bigger sphere. A test with 120°C and an Ø11 mm sphere showed that this temperature was too high for the process. As it can be seen in Fig. 41, the depth of grooves is significantly deeper compared to other temperatures since the temperature difference between 100°C and 120°C is smaller compared to 75°C and 100°C. This significant increase indicates that plastic is melted, and the process is close to soldering than forming. Wrinkles, loose filaments, and coarse surface of the path were observed. It was also decided not to experiment with the same temperature but a bigger sphere due to the inapplicability. However, approaches with 75°C and 100°C forming temperatures showed positive results. Grooves formed with an Ø11 mm sphere under 75°C condition are notable to the naked eye and has smooth surfaces without edgy contours. The same output was acquired with a bigger forming ball. As results revealed, the maximum depth of groove with Ø11 mm sphere at 75°C and 500N force is equal to 0,0197mm and with a Ø12,5 mm forming ball under same conditions – 0,015 mm. These results are similar to 100°C and 300N force static research conditions. Compared to previously performed static investigation, grooves are more trivial in dynamics: 0,0087 mm < 0,1301 mm (300N, 75°C, Ø11 mm) and 0,0066 mm < 0,0984 mm (300N, 75°C, Ø12,5 mm,). This evaluation proves that in the process of forming, the faster the tool moves, the less formable polymer is due to lower heat absorption in time. Under 100°C, grooves are more notable: under 300N, 400N, and 500N applied force, edgy contours of imprints are notable – incremental forming under this temperature would be inaccurate under the same experimental speed. Also, under 100°C, wrinkles are generated at the point where the static condition transforms into dynamic movement. This phenomenon creates a difficult problem where a greater amount of heat is transferred to a unit of sheet volume at the start and end of the process when the tool is stationary. Observation of the process revealed that the sphere of the forming tool is not rotating in the dynamic process. This defect is possible due to the stronger magnetic forces created by the magnet than a friction force between the ball and the sheet. Overall, the dynamic approach allowed to set narrower boundaries of the self-heating tool's sphere temperature – the best temperate for incremental forming under 6,33 mm/s is between 75°C and 100°C. However, the experiment raised a problem – proper selection of forming sphere's temperature and forming speed to ensure the best quality and effectiveness ratio. Acquired data of dynamic investigation will be used to simulate the incremental polymer sheet forming process.

## 4. Simulation of Forming Forces on a Polymer Sheet

A novel self-heating tool simulation approach is created to find the best parameters for incremental forming. The simulation helps to find essential variables values for the most effective process, reveals temperature and stress distribution in the material, and predicts the outcome of the forming. This chapter presents ANSYS calculations of held static investigation of a self-heating forming tool.

### 4.1. Thermal Simulation of Temperature Distribution

Since experimental research was conducted on temperature distribution in polymer layers, a simulation can be generated to obtain mechanical results of the material. All factors that influenced static investigation results must be included in this calculation to create an accurate simulation. Properly chosen material and its characteristics play a huge part in the validity of calculations. Polymer PVC Trovidurv ESA-D and a steel forming ball were used in every experiment. Properties of the plastic material are provided in Table 4. All characteristics of the material are provided in Appendix 6.

**Table 4.** Properties of PVC Trovidurv ESA-D polymer material

Parameter	Value	Unit
Density	1,41	g/cm <sup>3</sup>
Tensile modulus of elasticity	2500	MPa
Coefficient of linear thermal expansion	60 – 80	10 <sup>-6</sup> / K
Service temperature	-30 ... 60	°C
Yield stress	45	MPa

However, not all needed characteristics of polymer are provided by the material supplier. To obtain needed information such as yield strength and plastic strains at different material temperatures Research Project's no. 2 experimental stress-strain curves (obtained by the author) were used. For isotropic thermal conductivity and specific heat, average values for PVC polymer were used since values vary due to material composition. Isotropic thermal conductivity is equal to 0,15 W/mK [34] and specific heat – 880 J/(Kg °C) [35]. Data with created material specifications used in the ANSYS simulation is shown in Fig. 42.

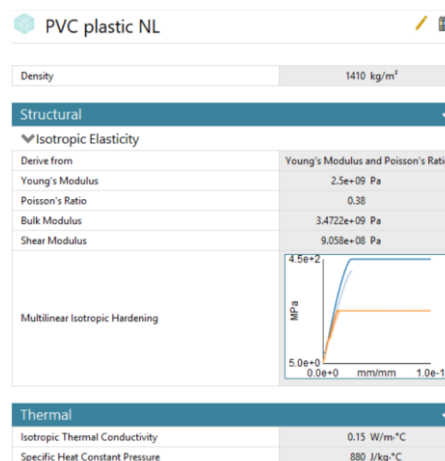


**Fig. 42.** Properties of PVC Trovidurv ESA-D material in ANSYS Library

A simulation was created to calculate the temperature distribution in polymer samples when the forming ball is tangent to the sheet's surface. The simulation was simplified by investigating only half of the sphere and polymer sheet in the ANSYS environment. Calculations were done with 50°C, 60°C, 75°C, and 90°C temperatures together with Ø12,5 mm sphere and 22°C 3 mm thickness sample. The symmetry region was used on the model to maintain a real case. Quad Hex Dominant finite element mesh method with the size of single element size equal to 0,25 mm was used to solve the problem. Initial conditions of investigation are shown in Fig. 43 and Fig. 44.

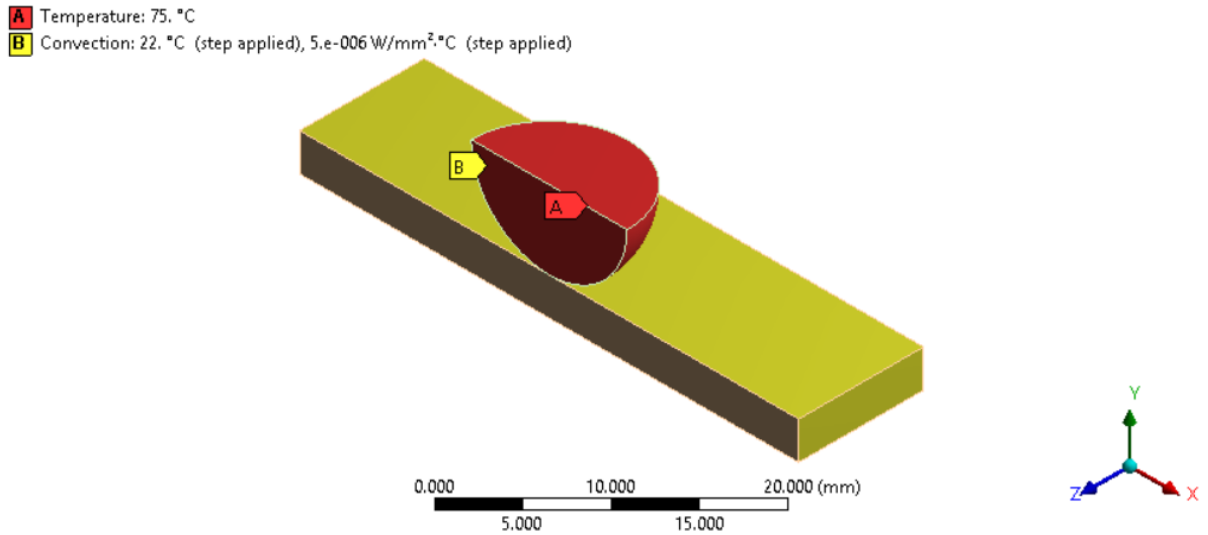


**Fig. 43.** Initial conditions of thermal simulation

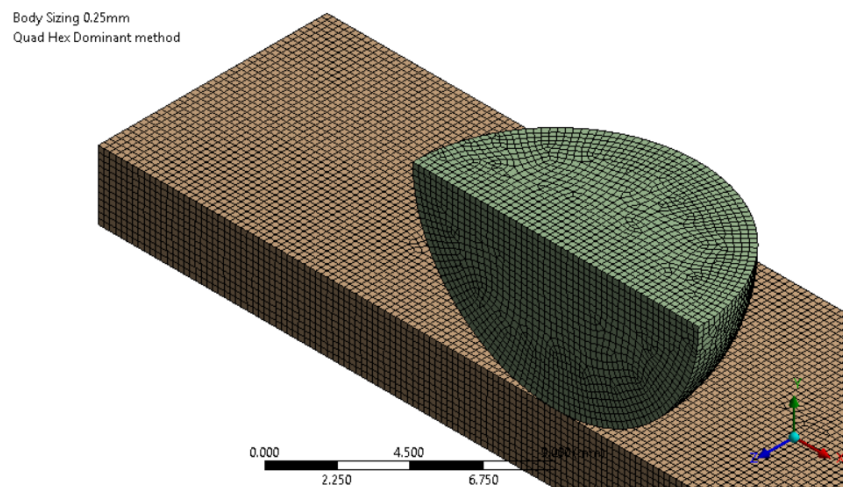


**Fig. 44.** Quad Hex Dominant mesh with a size of single element size of 0,25 mm

Calculated heat distribution in the sheet under a specific temperature is shown in Fig. 45. Results of the simulation are shown in Fig. 46. The graph shows that simulation temperatures in deeper layers with all forming ball temperatures are lower than the measured ones in the static experiment. An exception is the farthest material point. Experimental values in 3 mm at all temperatures are lower than experimental.

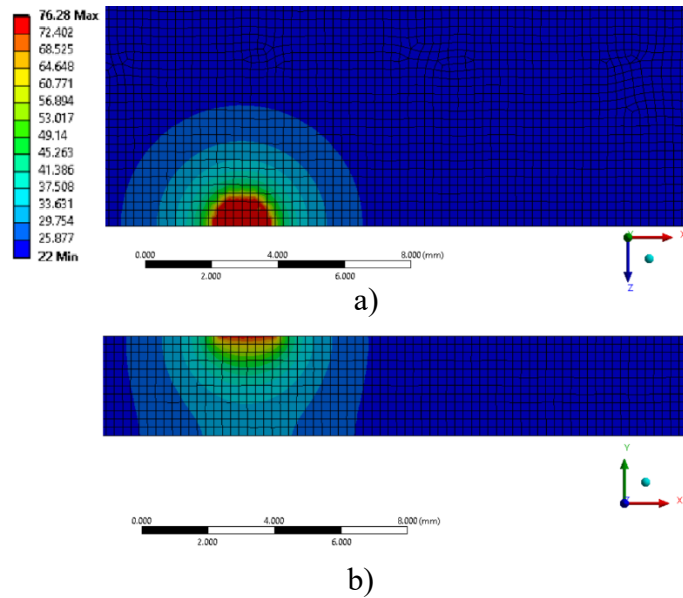


**Fig. 45.** Temperature distribution in a sheet while affected with 75°C forming ball: a) top view, b) front view

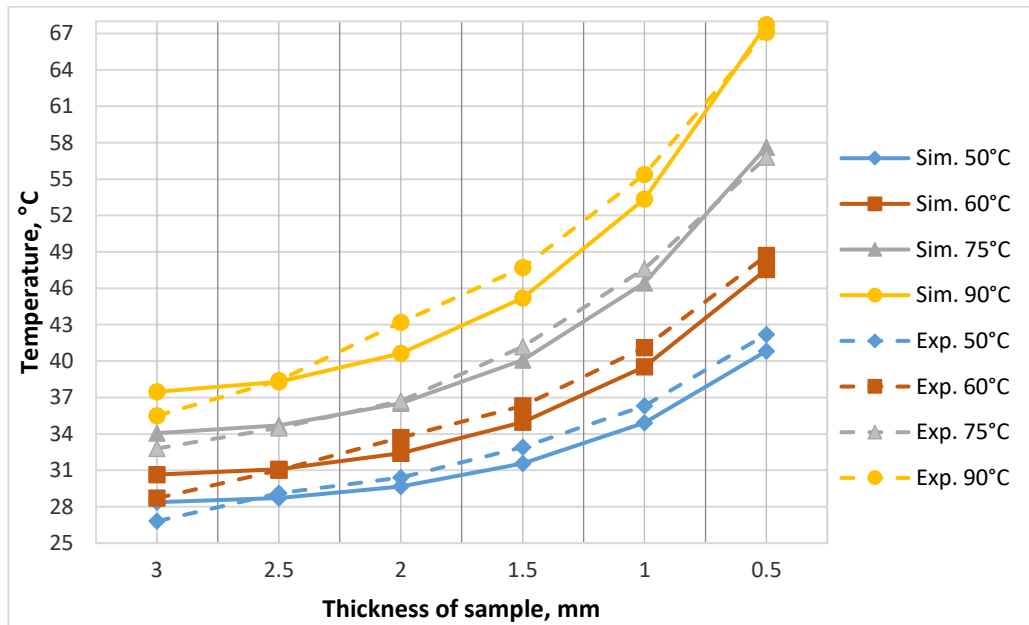


**Fig. 46.** Simulated temperature values of sheet layers under different forming ball temperatures versus thickness of a sheet

The comparison between experimental and simulation results revealed that in 0,5 mm thickness of the sheet, temperature values differ by 1%. Simulation values are close to experimental values, and calculations are approved as valid. However, data is not identical due to measurement errors and material properties discrepancies. Thermal simulation results are implemented in further static structural analysis.

#### 4.2. Static Structural Simulation of Forming Forces

The static simulation approach is the first step in simulating the SPIF process with a self-heating tool. The same model as in thermal analysis is used for this approach. Calculations were done with 50°C, 75°C, and 100°C temperatures together with Ø12,5 mm forming ball and forces equal to 100N, 200N, and 300N, as in the static experiment. The simulation was created to calculate the depth of imprints

formed under different temperatures and forces. Quad Hex Dominant FE mesh method with the size of single element size equal to 0,2 mm was used to solve the problem. Initial conditions of investigation are shown in Fig. 47 and Fig. 48.

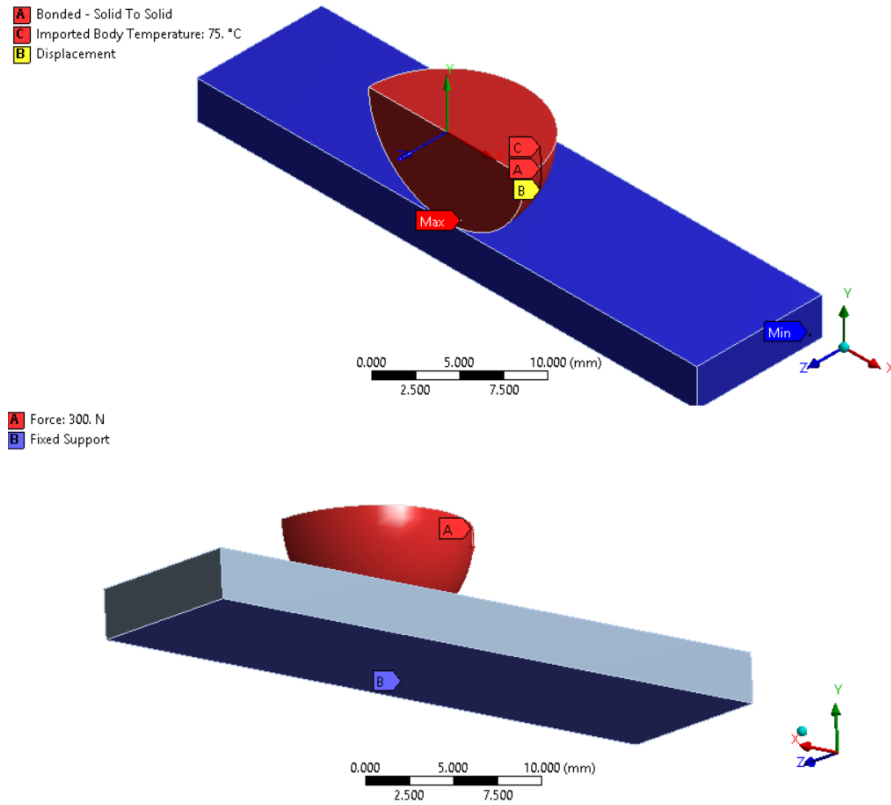


**Fig. 47.** Initial conditions of static structural simulation

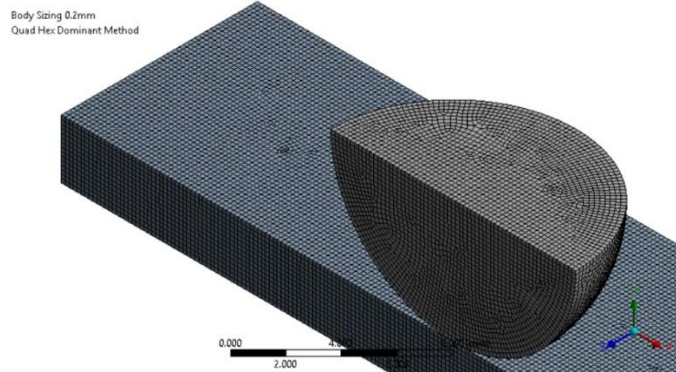


**Fig. 48.** Quad Hex Dominant mesh with a size of single element size of 0,2 mm

Thermal calculations were inserted into the model to conduct a proper simulation. Bonded contact mode “solid to solid” was used since the endpoint of the sphere has continuous contact. Force was applied on the sphere’s flat surface. All degrees of freedom of the sphere were constrained except movement in Y-axis. The sample was fixed with a whole lower surface. Calculated displacements of the sheet in millimeters under 300N force are shown in Fig. 49. Results of the simulation – depth of imprint values under 12,5 mm forming ball diameter and different temperatures versus applied forces are shown in Fig. 50.

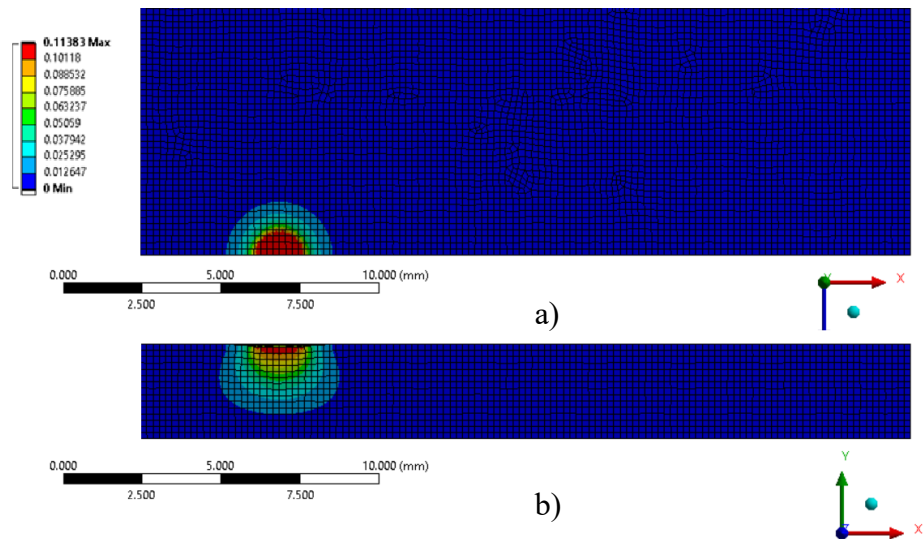


**Fig. 49.** Displacements of the sheet while affected with 75°C forming ball and 300N force: *a)* top view, *b)* front view

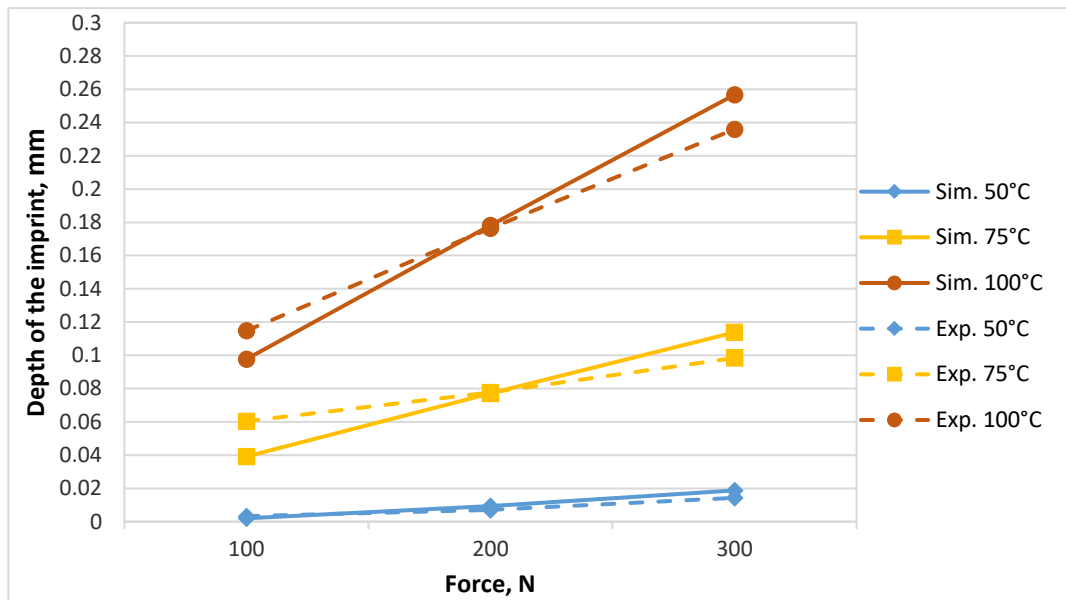


**Fig. 50.** Simulated depth of imprint values under 12,5 mm forming ball diameter and different temperatures versus applied forces

The comparison between experimental and simulation results revealed that under 300 N force and 75°C ball temperature 0,5, imprint values differ by 15%. Simulation values are close to experimental values, and calculations are approved as valid. However, data is not identical due to measurement errors and material properties discrepancies. A created model with thermal and mechanical properties provides a strong background for further dynamic simulation of the impact. The validity of dynamic simulation can be checked by comparing the depth of grooves with dynamic investigation results.

## 5. Robotic Incremental Forming of Polymer Sheet

After investigating heating element and self-heating tool possibilities, obtained data is used to perform an incremental robotic forming of polymer sheet using a designed single point self-heating tool. Previous research provided valuable information about the distribution of temperatures in polymer, forces and temperatures influence on formability and quality, and proved that sphere size and feed rate influence forming. With acquired knowledge through experimental research, the incremental forming process is performed. Further in this chapter, the incremental forming process is performed under different forming speeds, forming ball sizes, and lubrication conditions to find quality dependencies on these parameters. Results are compared to other authors' investigations.

### 5.1. Experimental Background

Two different size spheres were investigated to find a geometrical influence on the part's surface finish. The process was performed with a 75°C temperature forming ball since previous experiments showed that T<sub>g</sub> temperature of PVC polymer could be reached with this amount of heat. Three speeds of ABB IRB1200 robot were researched: 18,3 mm/s, 54,5 mm/s and 73 mm/s. Step of gradual downgrading – 0,5 mm. Round cylindrical samples with a 45° wall angle were formed in the process. The thickness of the sheet – is 2 mm. The principle of the process and initial variables are shown in Fig. 51.

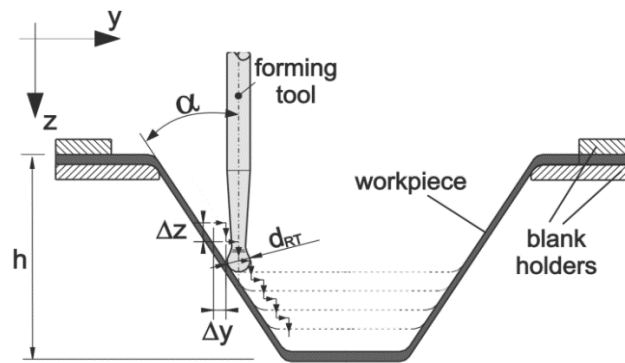


**Fig. 51.** Essence of held incremental forming process and main variables:  $\Delta z = 0,5$  mm,  $\Delta y = 0,5$  mm,  $d_{RT} = 12,5$  mm and 11 mm,  $\alpha = 45^\circ$ ,  $h = 30$  mm [36]

Self-heating tool is programmed to move in circles by reducing its perimeter by  $\Delta y = 0,5$  mm. Every circle drawn by the tool is lower in the Z-axis by  $\Delta z = 0,5$  mm. Since both steps are equal, wall angle  $\alpha = 45^\circ$  is formed. The formed part's height  $h$  is generated when the biggest and smallest circles are described in the program. The Height of the part set in the program is equal to 30 mm in this approach. Two different diameter  $d_{RT}$  forming balls were used: 11 mm and 12,5 mm. Literature analysis revealed that the best process quality of 2 mm and 3mm PVC polymer sheets is achievable with  $\Delta z = 0,5$  mm [37]. Authors report that the cause-effect relation in PVC polymer sheets is to decrease sheet thickness to increase formability. Authors report that maximum formability is at  $\alpha = 72^\circ$ , nominal feed rate 25mm/s, tool diameter  $d_{RT} = 10 - 15$  mm [38], while cause-effect relation is to increase tool diameter to increase formability [37]. The schematic view of an investigated incremental forming process is shown in Fig. 52 (left) and the set-up view in Fig. 52 (right).



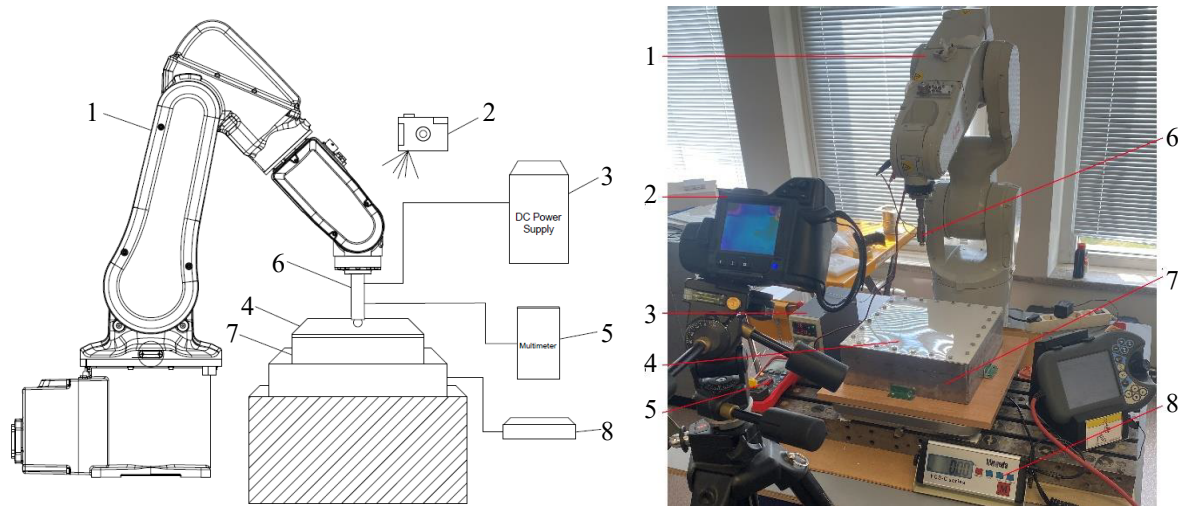


**Fig. 52.** Process investigation schematic view (left), set-up view (right). 1 – Manipulator ABB IRB1200 (ABB Robotics & Discrete Automation, Västerås, Sweden), 2 – Thermal imaging camera FLIR T450sc (Teledyne FLIR LLC, USA), 3 – DC Power Supply HY1803D (Mastech Digital, Inc., USA), 4 – PVC ESA-D 2mm thickness polymer sheet, 5 – Digital Multimeter (Uni-Trend Technology Co., Ltd., China), 6 – Designed SPIF self-heating tool, 7 – Holding frame, 8 – FCS-C series platform scales (UAB Mingeda, Lithuania)

Self-heating forming tool (6) is attached to manipulator ABB IRB1200 (1). 2 mm thickness blank (4) is clamped to the blank holder (7). The blank holder is rigidly attached to FCS-C platform scales (8) which indicates the weight of forming forces. DC Power Supply HY1803D (3) provides the necessary power to maintain the forming ball's temperature at 75°C. Digital Multimeter Uni-Trend (5) was used to track the temperature of the forming sphere, and thermal imaging camera FLIR T450sc (2) to track the temperature on the blank. The forming process proved that forming ball is not rotating as in the experimental research. The friction force between the forming ball and polymer sheet is lower than generated magnetic forces. As the solution, magnetic forces should be investigated, and a solution to insert a low friction gasket between the magnet and a ball should be proposed. Initiated robot program is provided in Appendix 7. Four different samples were formed in the process under different parameters. Taken approaches with conditions are listed in Table 5.

**Table 5.** Initial conditions of a held experiment

Approach no.	The temperature of the ball, °C	Diameter of the ball, mm	Feed rate, mm/s	Step size, mm	Lubricant
1.	75	12,5	73	0,5	None
2.	75	11	54,5	0,5	None
3.	75	11	18,3	0,5	None
4.	75	11	73	0,5	Motor oil HD 30

It was decided to keep the ball's temperature in research constant since the sheet surface temperature can be measured with a thermal imaging camera. A constant temperature in this investigation allows us to evaluate variables' influence on formability and quality.



## 5.2. Results of Robotic Incremental Forming Approach

This section presents the results of the robotic incremental forming investigation. Results are divided into two subsections. The first one describes acquired data about temperature distribution on the sheet, formability, and the actual height of the part. The second part presents a quality evaluation of samples. Samples after the process are shown in Fig. 53.

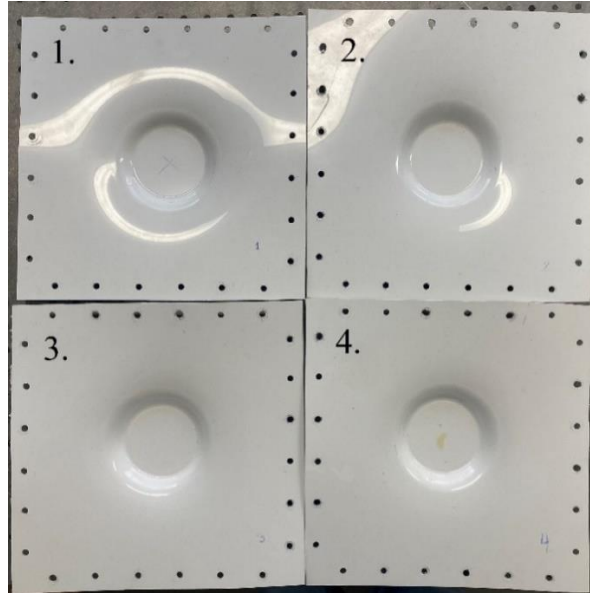


**Fig. 53.** Samples after the SPIF process: 1. Ball diameter 12,5 mm, feed rate 73 mm/s, lubricant – none, 2. Ball diameter 11 mm, feed rate 54,5 mm/s, lubricant – none, 3. Ball diameter 11 mm, feed rate 18,3 mm/s, lubricant – none 4. Ball diameter 11 mm, feed rate 73 mm/s, lubricant – motor oil

### 5.2.1. Formability

Static experiment and simulation proved that a 75°C forming ball can heat PVC polymer plastic to 56°C temperature. The dynamic approach revealed that forming ball temperature in the process should be between 75°C and 100°C to heat the polymer efficiently. However, the first approach was taken with the lowest provided temperature – 75°C. This selection is explained by the high speed of forming tool and the high repeatability of heating the same unit of volume at a high frequency. Temperature distribution in polymer sheet after the process is shown in Fig. 54.

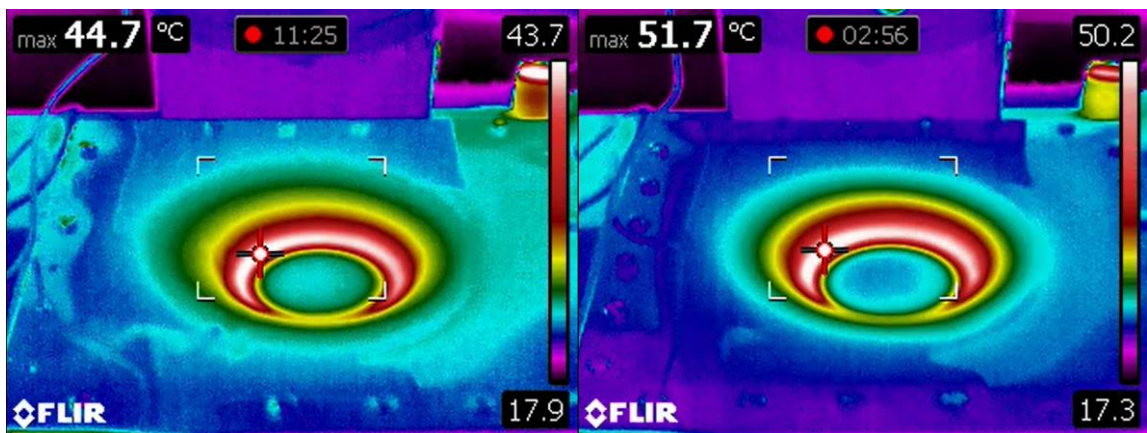


**Fig. 54.** Data acquired through thermal imaging camera FLIR T450sc. Feed rate 18,3 mm/s., 44,7°C (left), feed rate 73 mm/s., 51,7°C (right)

Results proved that the sheet's temperature under a constant temperature of the sphere is directly dependent on forming speed. Investigation revealed that a higher heating frequency is more effective even if a ball heats one unit of polymer's volume for a shorter period. Polymer's surface temperature dependence on feed rate is shown in Fig. 55.

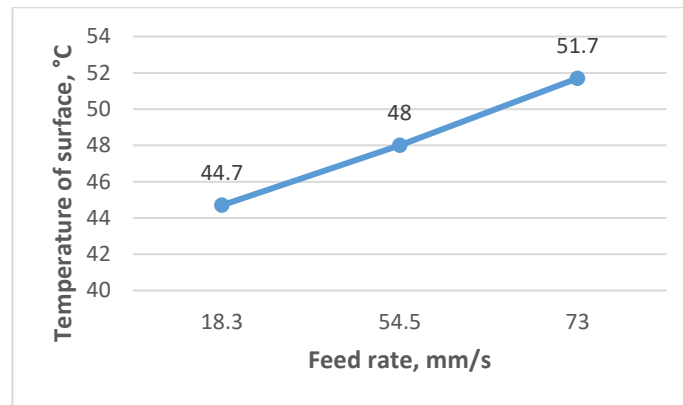


**Fig. 55.** Polymer's surface temperature dependence on feed rate

Literature provides that forming force is dependent on tool diameter, the thickness of the sheet, tool speed, and step size [37]. The authors state that increase in tool diameter increases forming forces. Results showed that under the same conditions, maximal forming force increased by 9N when a bigger sphere was used (from 442N to 451N). Authors claim that decrease in forming speed decreases forming forces [37]. An experiment showed the exact outcome. Forming forces dependency on forming speed under the same conditions is shown in Fig. 56. This graph provides valuable information since different temperatures should affect the perpendicularity of the curve and values as well, as previous experiments revealed. Increasing the tool's temperature should reduce the angle of perpendicularity and values of forming forces.

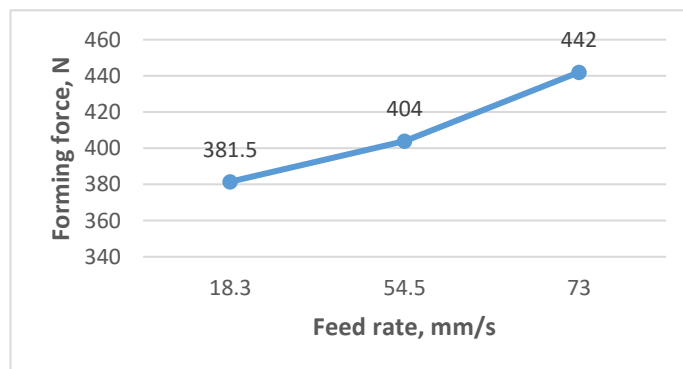


**Fig. 56.** Forming force dependence on feed rate under same initial conditions

Another parameter that can be evaluated and compared is height of the formed part. As mentioned before, the theoretical height of the formed part is 30 mm. Due to elastic deformations, spring-back effect, and other phenomena, the experimental height of parts differ. As seen in Fig. 57, the highest part was formed with 54,5 mm/s speed. Results revealed that under 73 mm/s speed and Ø12,5 mm forming ball achieved height is equal to 22,2 mm, and under 73 mm/s speed and Ø11 mm – 23,9 mm. This observation proves that the higher formability of part is achievable with a smaller sphere.

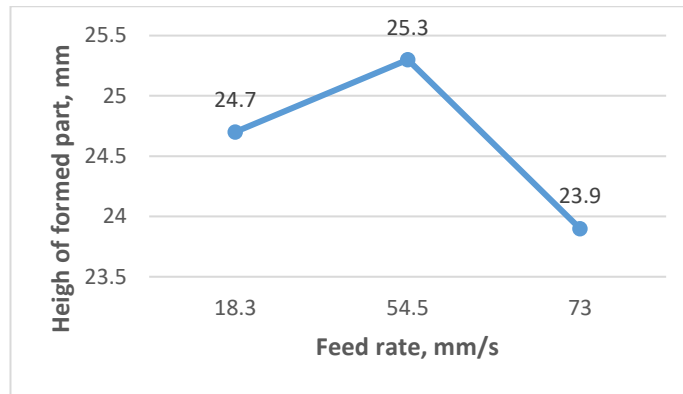


**Fig. 57.** Formed height of part dependence on feed rate under same initial conditions with Ø11 mm forming ball

However, investigation results revealed that the temperature of a sheet surface should be higher to increase formability. Analyzed experimental data gave valuable information about temperature, forces, and depth dependencies on formability. However, experimenting with higher temperatures should reveal the best temperature-speed ratio. Higher temperature should also reduce forming forces. Research revealed that optimal feed rate could increase formability, obtain close results to theoretical height of formed part, system off-set should be made.

### 5.2.2. Quality

To obtain the performance results of the process, it is necessary to evaluate the quality of the formed part. High surface quality and no errors is a required property in the ISPF process. In this approach, the surface finish is measured by a portable roughness tester. The procedure of roughness measuring is shown in Fig. 58. Measurements were completed under room temperature and repeated five times, and average values are shown as results.

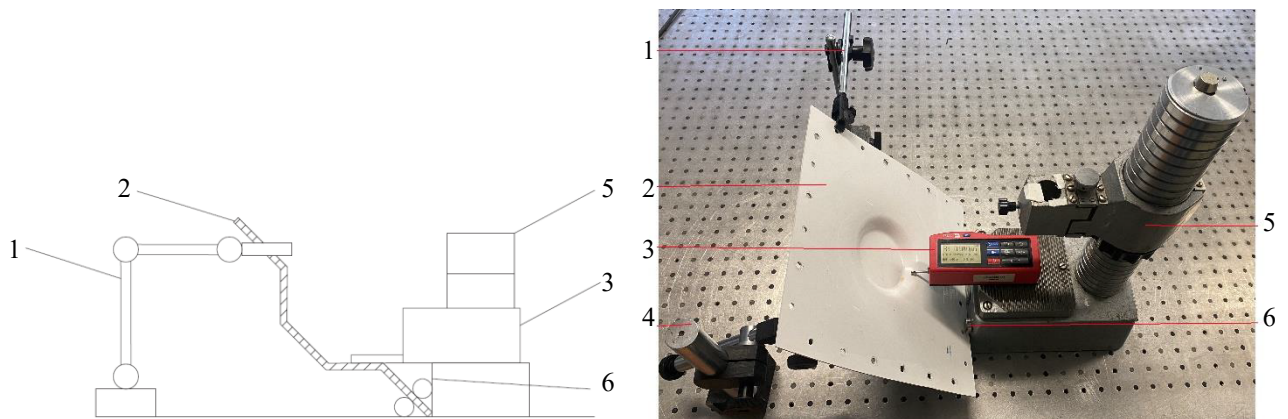


**Fig. 58.** Set-up schematic view of surface roughness measurements (left), set-up view (right). 1 – Clamp, 2 – Formed part, 3 – Roughness tester with graphical display TR220 (Beijing TIME High Technology Ltd., South Korea), 4 – Clamp, 5 – Stand, 6 – Magnet

Formed part (2) was attached to two clamps (1, 4) on one side. The other side of the blank was restrained with magnets (6). The polymer was positioned at 45° to make forming brim parallel to the base. A portable roughness tester (3) was placed on the stand, and its indicator was carefully placed on the polymer's brim. Measurements were performed on different points of the sample each time. Measured values are listed in Table. 6.

**Table 6.** Measured values of surface roughness under different experimental conditions

Approach no.	Diameter of the ball, mm	Feed rate, mm/s	Lubricant	Average roughness Ra, $\mu\text{m}$	The maximum peak of the valley height Rz, $\mu\text{m}$
1.	12,5	73	None	0,083	0,3588
2.	11	54,5	None	0,0906	0,3836
3.	11	18,3	None	0,1006	0,4412
4.	11	73	Motor oil HD 30	0,0506	0,3198

Results revealed that the size of the forming ball influences surface finish. Average roughness Ra and a maximum peak of grooves Rz are higher with a smaller sphere. Cause-effect relation: increase the size of the forming ball increases surface quality. Results showed that feed rate influences quality. Cause-effect relation: to increase speed to increase surface quality. Approach taken with a motor oil lubricant showed positive results on surface quality. Ra parameter increased by 79% and Rz by 20% compared to the 54,5 mm/s approach. Authors of similar conducted research [39] on PVC ISPF process state that under step size 0,5 mm, tool diameter 10 mm, feed rate 25 mm/s, and sheet thickness 2 mm, Ra was equal to 0,405  $\mu\text{m}$  and maximum forming forces 554.68 N [39]. This force is 25,5% greater than the self-heating tool's maximum force at a 73 mm/s feed rate. The novel tool creates lower forces in the process, and this way, the overall power consumption is lower. Local heating with a novel tool in this approach required only 2,7 W to maintain the 75°C temperature of the forming ball. Literature research showed similar assisted by heating ISPF experiments were held with local heating equipment whose maximum power is 2000W [32]. Local heating requires less power since less heat is radiated into the environment, and heat is more concentrated into one unit of material's volume.

## Conclusions

1. A self-heating forming tool for the incremental single point forming process was designed. The tool's design includes a 60 W soldering-iron heat element inserted into a steel shell with textolite bushings, a PID temperature controller with a solid-state relay, a thermocouple attached to the tool, and a power supply. The heating process investigation reveals that under the 75°C sphere's temperature, polymer temperature in 0,5 mm thickness of the sheet reaches 56,8°C temperature close to optimal processing temperature. 2,7 W of power was used to reach this temperature.
2. Experimental research on the designed self-heating tool was conducted. Results of static and dynamic experiments of the designed self-heating tool revealed that the depth of the groove is directly proportional to applied force under the same size forming ball and the smaller the sphere's diameter is, the deeper imprint is. Results of the static experiment showed that increasing temperature from 50°C to 75°C increases formability 3,72 times, and from 75°C to 100°C increases formability 2,3 times. Approaches with 75°C and 100°C forming temperatures show positive results: grooves are notable to the naked eye and have smooth surfaces. Formability between these values increases by 63,3%. Dynamic research sets temperature boundaries at 75-100°C for further research.
3. A simulation of heated tool incremental forming forces on polymer sheet was made. This simulation is a simplified calculation of the polymer's temperature distribution and imprint depth. The comparison between experimental and simulation reveals that in 0,5 mm thickness of the sheet, temperature values differ by 1% and imprint values on the sheet's surface differ by 15% due to the measuring errors and mechanical properties discrepancies. The case simulation shows valuable information about stresses, thermal stresses, temperatures, and forces distribution in the case. A created model with thermal and mechanical properties provides a strong background for further dynamic simulation of the impact.
4. A robotic incremental forming of polymer sheets using a developed single point heating tool was performed. Results prove that the sheet's temperature is directly dependent on forming speed, an increase in tool diameter increases forming forces, and a decrease in forming speed decreases forming forces. The findings are exact to those found by other authors [37]. The higher formability of part is achievable with a smaller sphere: under 73 mm/s speed and Ø12,5 mm forming ball achieved height is equal to 22,2 mm, and under 73 mm/s speed and Ø11 mm – 23,9 mm of set 30 mm. Results reveal that the forming ball's size, feed rate, and lubrication influence surface finish: increase the size of the forming ball to increase surface quality, increase speed to increase surface quality.

## **Recommendations**

Completed research not only answered many questions but raised new ones. An ISPF process with a novel self-heating has the potential to achieve high quality and formability. However, more research must be done. Recommendations for future investigation are provided below.

1. To investigate magnetic forces generated by magnet and redesign self-heating tool with a solution of rotating ball. As it is now, the friction force between the sheet and sphere is lower than the magnetic force. High thermal conductivity and frictionless gasket could be used between the magnet and forming ball.
2. To improve the self-heating tool with a force sensor to maintain constant forming force. Constant force should ensure even forming and distributed stresses. Compare formability with previous results.
3. To perform a dynamic simulation approach. The next step in approaching the incremental process with a novel tool is dynamic calculations in the ANSYS environment under exact conditions as held dynamic experiment. Gained data should be compared to experimental results.
4. To perform SPIF investigation with a novel tool under different temperatures of the forming ball. Experiments should be performed under the same conditions to compare outcomes. Results should reveal the best temperature-speed ratio. Higher temperature should also reduce forming forces.
5. To perform experimental research on maximum formability with the most optimal parameters. To evaluate maximum wall angle, depth of the part, and occurred error types. Compare results with other authors' research.

## List of references

1. KUMAR, Ajay; GULATI, Vishal; KUMAR, Parveen. Investigation of surface roughness in incremental sheet forming. *Procedia computer science*, 2018, 133: 1014-1020.
2. PANDRE, Sandeep, et al. Processing of DP590 steel using single point incremental forming for automotive applications. *Materials and Manufacturing Processes*, 2021, 36.14: 1658-1666.
3. ROSENTHAL, Stephan, et al. Lightweight in automotive components by forming technology. *Automotive Innovation*, 2020, 3.3: 195-209.
4. BARIMANI-VARANDI, Abozar; NASRABADI, Mohammad Kazemi; RAVAN, Bahram Abedi. Feasibility study of single point incremental forming of aircraft canopy for polycarbonate sheet. *Amirkabir*, 2021.
5. SBAYTI, M., et al. Optimization techniques applied to single point incremental forming process for biomedical application. *The International Journal of Advanced Manufacturing Technology*, 2018, 95.5: 1789-1804.
6. BOULILA, Atef, et al. Contribution to a biomedical component production using incremental sheet forming. *The International Journal of Advanced Manufacturing Technology*, 2018, 95.5: 2821-2833.
7. CHENG, Zinan, et al. Incremental sheet forming towards biomedical implants: A review. *Journal of Materials Research and Technology*, 2020, 9.4: 7225-7251.
8. ZHANG, Danning; HEIDER, Dirk; GILLESPIE JR, John W. Void reduction of high-performance thermoplastic composites via oven vacuum bag processing. *Journal of Composite Materials*, 2017, 51.30: 4219-4230.
9. MA, Yijia; CENTEA, Timotei; NUTT, Steven R. Defect reduction strategies for the manufacture of contoured laminates using vacuum BAG-only prepregs. *Polymer composites*, 2017, 38.9: 2016-2025.
10. CHEN, Fei; ZHAN, Lihua; LI, Shujian. Refined simulation of temperature distribution in molds during autoclave process. *Iranian Polymer Journal*, 2016, 25.9: 775-785.
11. PATIL, Jeet P., et al. Transient thermal analysis of close pressure thermoforming process. *Journal of Manufacturing Processes*, 2021, 62: 513-522.
12. LEITE, Wanderson De Oliveira, et al. Vacuum thermoforming process: an approach to modeling and optimization using artificial neural networks. *Polymers*, 2018, 10.2: 143.
13. STANSBURY, Jeffrey W.; IDACAVAGE, Mike J. 3D printing with polymers: Challenges among expanding options and opportunities. *Dental materials*, 2016, 32.1: 54-64.
14. FERNANDES, Célio, et al. Modeling and Optimization of the Injection-Molding Process: A Review. *Advances in Polymer Technology*, 2018, 37.2: 429-449.
15. TRZEPIECIŃSKI, Tomasz, et al. Emerging trends in single point incremental sheet forming of lightweight metals. *Metals*, 2021, 11.8: 1188.
16. MCANULTY, Tegan; JESWIET, Jack; DOOLAN, Matthew. Formability in single point incremental forming: A comparative analysis of the state of the art. *CIRP Journal of Manufacturing Science and Technology*, 2017, 16: 43-54.
17. JESWIET, J., et al. Asymmetric single point incremental forming of sheet metal. *CIRP annals*, 2005, 54.2: 88-114.
18. SILVA, M. B.; MARTINS, P. A. F. Two-point incremental forming with partial die: theory and experimentation. *Journal of Materials Engineering and Performance*, 2013, 22.4: 1018-1027.

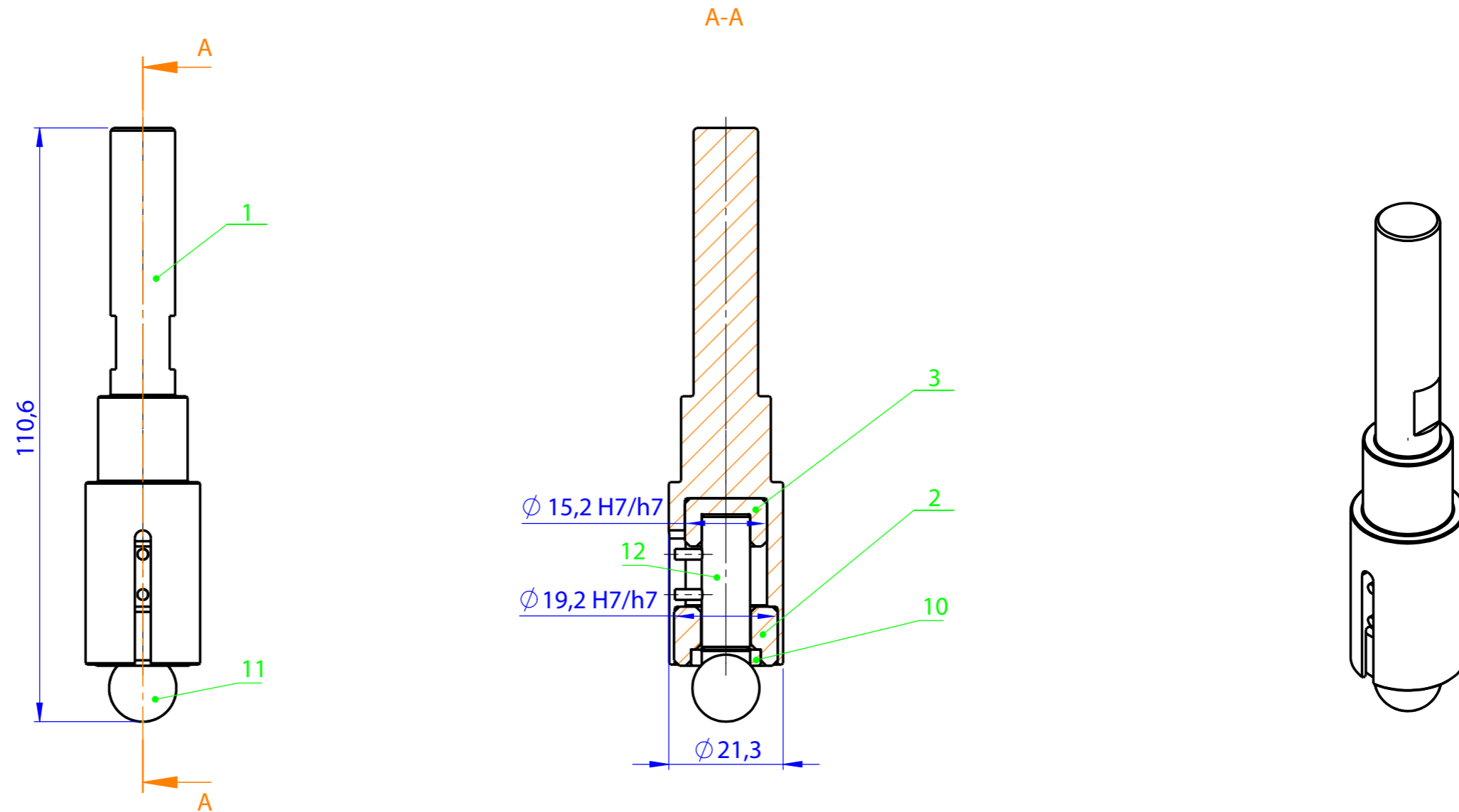
19. PENG, Wenxuan; OU, Hengan; BECKER, Adib. Double-sided incremental forming: a review. *Journal of Manufacturing Science and Engineering*, 2019, 141.5.
20. DOS SANTOS, W. Nunes; DE SOUSA, J. A.; GREGORIO JR, R. Thermal conductivity behaviour of polymers around glass transition and crystalline melting temperatures. *Polymer Testing*, 2013, 32.5: 987-994.
21. BAYERL, Thomas, et al. The heating of polymer composites by electromagnetic induction—A review. *Composites Part A: Applied Science and Manufacturing*, 2014, 57: 27-40.
22. DAS, Sumana, et al. Prospects of microwave processing: An overview. *Bulletin of materials science*, 2009, 32.1: 1-13.
23. ABLIZ, Dilmurat, et al. Curing methods for advanced polymer composites-a review. *Polymers and Polymer Composites*, 2013, 21.6: 341-348.
24. US8033151B2 - method and apparatus for reducing force needed to form a shape from a sheet metal. *Google Patents* [online]. [Accessed 8 May 2022]. Available from: <https://patents.google.com/patent/US8033151B2/en?q=US8%2C033%2C151>
25. LI, Pengyang, et al. Evaluation of forming forces in ultrasonic incremental sheet metal forming. *Aerospace Science and Technology*, 2017, 63: 132-139.
26. DUFLOU, J. R., et al. Improved SPIF performance through dynamic local heating. *International Journal of Machine Tools and Manufacture*, 2008, 48.5: 543-549.
27. US7984635B2 - asymmetric incremental sheet forming system. *Google Patents* [online]. [Accessed 8 May 2022]. Available from: <https://patents.google.com/patent/US7984635B2/en?q=US7%2c984%2c635>
28. RCL. 2022. *ATIT17 PID temperatūros valdiklis TERMOSTATAS 400°C K-Type REX-C100 100-240V, SSR Output*. [online] [Accessed 8 May 2022]. Available from: <https://rcl.lt/products/atit17-pid-temperaturos-valdiklis-termostatas-400-c-k-type-rex-c100-100-240v-ssr-output>
29. RCL. 2022. *ATIT17 PID temperatūros valdiklis TERMOSTATAS 400°C K-Type REX-C100 100-240V, SSR Output*. [online] [Accessed 8 May 2022]. Available from: <https://rcl.lt/products/atit17-pid-temperaturos-valdiklis-termostatas-400-c-k-type-rex-c100-100-240v-ssr-output>
30. DAVYDOVA, I. F., et al. High-temperature inorganic glass textolites. *Glass and Ceramics*, 2014, 71.1: 60-63.
31. Thermtest Inc. n.d. *Thermal Conductivity of Steel*. [online] [Accessed 8 May 2022]. Available from: <https://thermtest.com/thermal-conductivity-of-steel>
32. OSTASEVICIUS, Vytautas, et al. Investigation of Advanced Robotized Polymer Sheet Incremental Forming Process. *Sensors*, 2021, 21.22: 7459.
33. DAVARPANAH, Mohammad Ali, et al. Effects of incremental depth and tool rotation on failure modes and microstructural properties in Single Point Incremental Forming of polymers. *Journal of materials processing technology*, 2015, 222: 287-300.
34. C-Therm Technologies Ltd. 2020. *The Thermal Conductivity of Unfilled Plastics – C-Therm Technologies Ltd.* [online]. [Accessed 8 May 2022]. Available from: <https://ctherm.com/resources/newsroom/blog/the-thermal-conductivity-of-unfilled-plastics>
35. C-Therm Technologies Ltd. 2020. *The Thermal Conductivity of Unfilled Plastics – C-Therm Technologies Ltd.* [online] [Accessed 8 May 2022]. Available from: <https://ctherm.com/resources/newsroom/blog/the-thermal-conductivity-of-unfilled-plastics>



36. ŻABA, Krzysztof, et al. ANALYSIS OF THE ALUMINIUM FORMABILITY IN THE INCREMENTAL SHEET FORMING PROCESS.
37. HASSAN, Malik, et al. Progress on single-point incremental forming of polymers. *The International Journal of Advanced Manufacturing Technology*, 2021, 114.1: 1-26.
38. FRANZEN, V., et al. Single point incremental forming of PVC. *Journal of materials processing technology*, 2009, 209.1: 462-469.
39. BAGUDANCH, I., et al. Forming force and temperature effects on single point incremental forming of polyvinylchloride. *Journal of materials processing technology*, 2015, 219: 221-229.



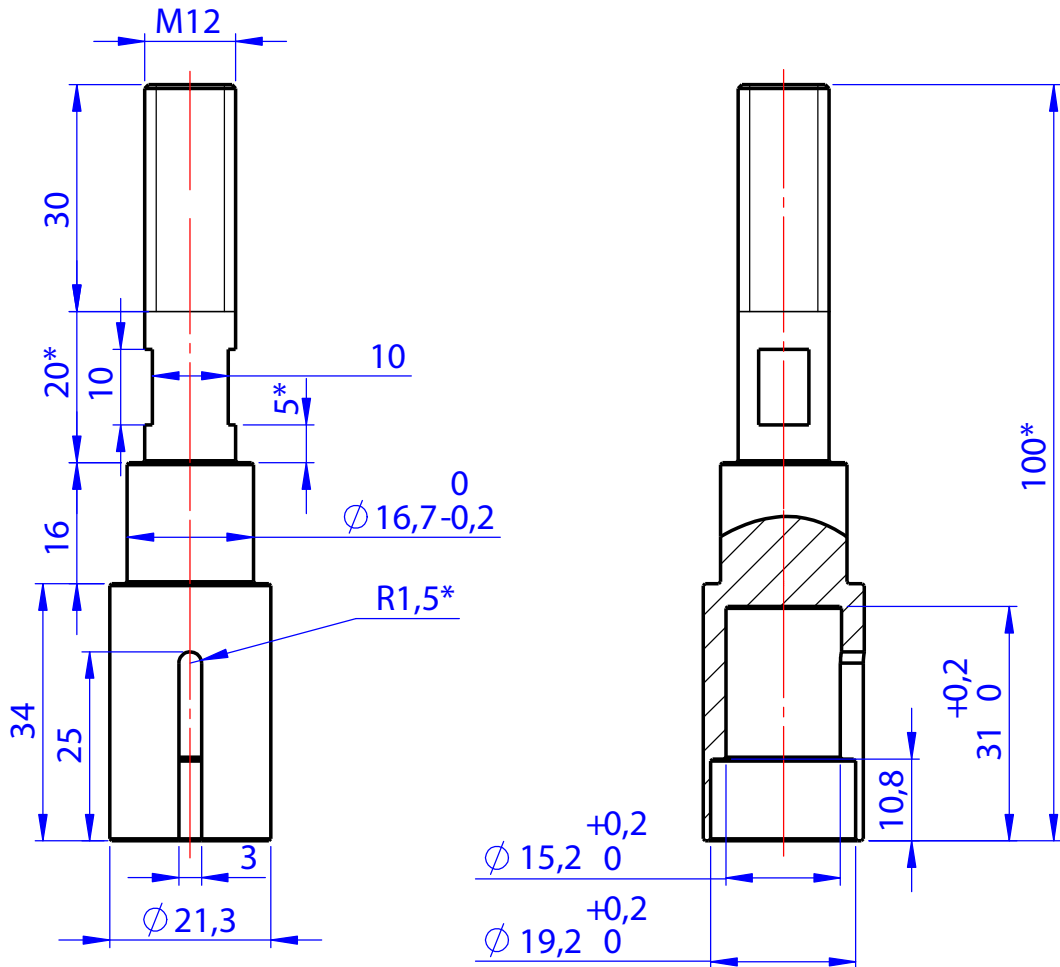
Appendix 2. Assembly drawing of Single point incremental forming heating tool



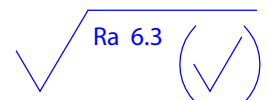
General tolerances as per LST EN 22768-mK

	File name	Additional information	Material	Scale 1:1
Resp. department MED	Technical reference	Document type Assembly drawing	Document status Training	
 kaunas university of technology 1922	Created by Baltramiejus Andrijaitis	Title, Supplementary title Single point incremental forming heating tool	SPIFT-00.00.000 AD	
	Approved by Darius Eidukynas		Rev. A	Date 2022-05-17

### Appendix 3. Drawing of the Tool

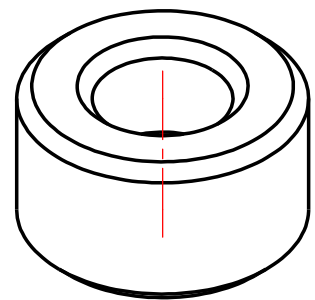
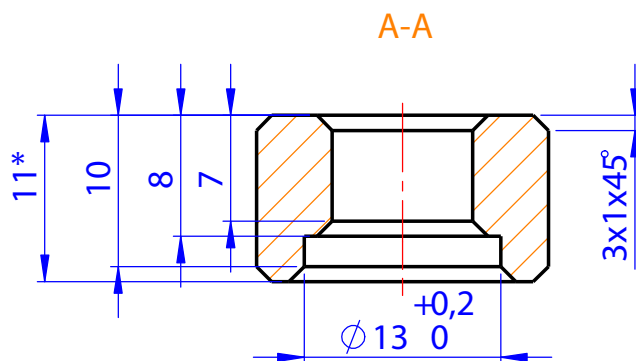
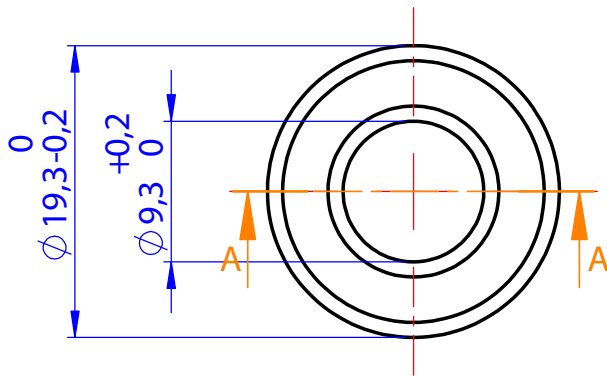


1. Unspecified tolerance limit according LST EN 22768-mK.
2. Unspecified radius of fillets  $R=0.25$  mm.†
3. \* - Informational dimensions

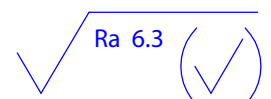


	File name	Additional information	Material Steel C45 LST EN 10083-1	Scale 1:1
Resp. department MIDF	Technical reference	Document type Part drawing		Document status Training
Legal owner 	Created by Baltramiejus Andrijaitis	Title, Supplementary title Tool		SPIFT-00.00.0.10
	Approved by Darius Eidukynas	Rev. A	Date 2022-05-17	Lang. En Sheet 1/1

## Appendix 4. Drawing of Textolite upper bushing

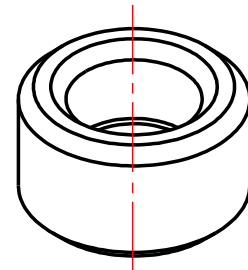
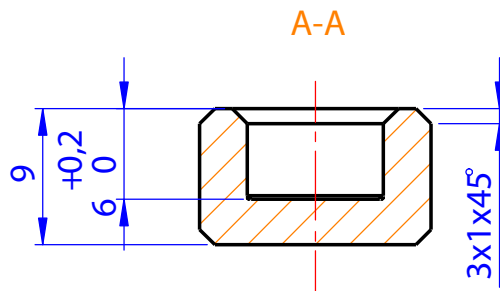
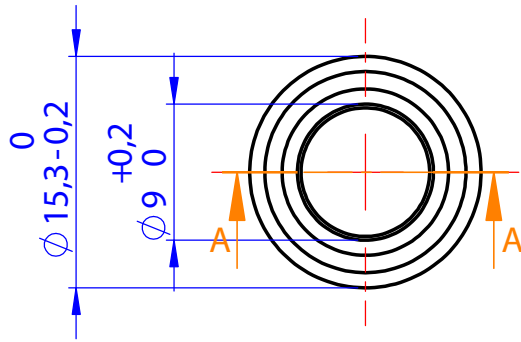


1. Unspecified tolerance limit according LST EN 22768-mK.
2. Unspecified radius of fillets  $R=0.5$  mm.
3. \* - Informational dimensions

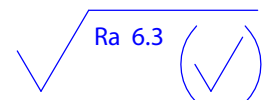


	File name	Additional information	Material <b>Textolite</b>	Scale <b>2:1</b>
Resp. department <b>MIDF</b>	Technical reference	Document type <b>Part drawing</b>	Document status <b>Training</b>	
Legal owner 	Created by <b>Baltramiejus Andrijaitis</b>	Title, Supplementary title <b>Textolite upper bushing</b>	<b>SPIFT-00.00.011</b>	
	Approved by <b>Darius Eidukynas</b>		Rev. <b>A</b>	Date <b>2022-05-17</b>
			Lang. <b>En</b>	Sheet <b>1/1</b>

## Appendix 5. Drawing of Textolite lower bushing



1. Unspecified tolerance limit according LST EN 22768-mK.
2. Unspecified radius of fillets  $R=0.5$  mm.
3. \* - Informational dimensions



	File name	Additional information	Material <b>Textolite</b>	Scale <b>2:1</b>
Resp. department <b>MIDF</b>	Technical reference	Document type <b>Part drawing</b>	Document status <b>Training</b>	
Legal owner  kauno technologijos universitetas 1922	Created by <b>Baltramiejus Andrijaitis</b> Approved by <b>Darius Eidukynas</b>	Title, Supplementary title <b>Textolite lower bushing</b>	<b>SPIFT-00.00.012</b>	
		Rev. <b>A</b>	Date <b>2022-05-17</b>	Lang. Sheet <b>En 1/1</b>

## Technical Data Sheet



### Trovidur® ESA-D

#### Product characteristics

- Highly impact resistant
- High UV and weather resistance
- Excellent printability

#### Product applications

- Construction industry
- Visual communication
- Vacuum forming industry

	Test method	Unit	Value
<b>General properties</b>			
Density	DIN EN ISO 1183-1	g / cm <sup>3</sup>	1,41
Water absorption	DIN EN ISO 62	%	≤0,20
Flammability (Thickness 1 ... 4 mm)	DIN 4102		B1
<b>Mechanical properties</b>			
Yield stress	DIN EN ISO 527	MPa	45
Elongation at break	DIN EN ISO 527	%	20
Tensile modulus of elasticity	DIN EN ISO 527	MPa	2500
Notched impact strength	DIN EN ISO 179	kJ / m <sup>2</sup>	8
<b>Thermal properties</b>			
Coefficient of linear thermal expansion	DIN 53752	10 <sup>-6</sup> / K	60 - 80
Service temperature, long term	Average	°C	-30 ... 60
Vicat softening temperature	DIN EN ISO 306, Vicat B	°C	75
<b>Electrical properties</b>			
Dielectric constant	IEC 60250		3,2
Dielectric dissipation factor (10 <sup>6</sup> Hz)	IEC 60250		0,02
Volume resistivity	IEC 60093	Ω * cm	>10 <sup>15</sup>
Surface resistivity	IEC 60093	Ω	>10 <sup>13</sup>

The data stated above are average values ascertained by statistical tests on a regular basis. They are in accordance with DIN EN 15860. The data above are provided purely for information and shall not be regarded as binding unless expressly agreed in a contract of sale.



## Appendix 7. Executed ABB robot incremental forming program

```
1. MODULE MainModule
2. VAR signaldo signaldo1;
3. !CIRCLE
4. !!!!!!!!!!!!!!!!!!!!! VARIABLE !!!!!!!!!!!!!!!!!!!!!!!!!!!!!
5.   !CONST num y0:=18.5;!initial position y (The center of circle)
6.   !CONST num x0:=512;!initial position x (The center of circle)
7.   CONST num y0:=-2.33;!initial position y (The center of circle)
8.   CONST num x0:=409.71;!initial position x (The center of circle)
9.   !CONST num z0:=250;!initil position z (top of center) aliuminis
10.  !CONST num z0:=325;!initil position z (top of center) plastikas
11.  CONST num z0:=355;!initil position z (top of center) plastikas su svarstyklemis
12.
13.  VAR bool ToStartPosition:= false;
14.  VAR bool ToStartCenter:= FALSE;
15.
16.  CONST num zdown:=0.5;!how much decrease of height every lap
17.  CONST num b:=0.5;!how much decrease of radius every lap
18.  CONST num Rmax:=70;!maximum radius
19.  CONST num Rmin:=40;!minimum radius
20.
21.  !VAR num z1:=z0-4;!height position of surface - !!!! sumazeja, pricarteja dar prie paviršiaus, reiketu + daryti
    arba didinti z0
22.  VAR num z1:=353.00;
23.  VAR num r1:=Rmax;!maximum radius
24.
25.  !!!!!!!!!!!!!!!!!!!!!!!!!!!!!!!!!!!!!!!!!!!!!!!!!!!!!!!!!!!!!!!!!!!!!!!!!!!!!
26.
27.  VAR num y1;!1st position y
28.  VAR num x1;!1st position x
29.  VAR num y2;!2nd position y
30.  VAR num x2;!2nd position x
31.  VAR num y3;!3rd position y
32.  VAR num x3;!3rd position x
33.  VAR num y4;!4th position y
34.  VAR num x4;!4th position x
35.  VAR num y5;!5th position y
36.  VAR num x5;
37.  CONST robtarjet jointmove0deg=[[432.99,-0.01,791.07],[0.707072,1.67775E-05,0.707142,2.46238E-06],[-1,-
    1,0,0],[9E+09,9E+09,9E+09,9E+09,9E+09,9E+09]];!5th position x
38.
39. PROC main()
40. !CIRCLE PROGRAM
41.   y1:=r1*sin(0)+y0;
42.   x1:=r1*cos(0)+x0;
43.   y2:=(r1-b/4)*sin(90)+y0;
44.   x2:=(r1-b/4)*cos(90)+x0;
```



```

45.   y3:=(r1-b/2)*sin(180)+y0;
46.   x3:=(r1-b/2)*cos(180)+x0;
47.   y4:=(r1-3*b/4)*sin(270)+y0;
48.   x4:=(r1-3*b/4)*cos(270)+x0;
49.   y5:=(r1-b)*sin(0)+y0;
50.   x5:=(r1-b)*cos(0)+x0;
51.
52.   IF ToStartCenter THEN
53.       MoveL [[x0,y0,z0],[0,0,1,0],[-1,-1,-1,0],[9E+09,9E+09,9E+09,9E+09,9E+09,9E+09]], v100, fine, tool0;
54.       WaitTime(5000);
55.   ENDIF
56.   IF ToStartPosition THEN
57.       MoveL [[x1,y1,z1],[0,0,1,0],[-1,-1,-1,0],[9E+09,9E+09,9E+09,9E+09,9E+09,9E+09]], v100, fine, tool0;
58.       WaitTime(5000);
59.   ENDIF
60.
61.   IF r1=Rmax THEN! (1)move to initial position (just touch surface)
62.       MoveL [[x0,y0,z0],[0,0,1,0],[-1,-1,-1,0],[9E+09,9E+09,9E+09,9E+09,9E+09,9E+09]], v100, fine, tool0;
63.       MoveL [[x1,y1,z1],[0,0,1,0],[-1,-1,-1,0],[9E+09,9E+09,9E+09,9E+09,9E+09,9E+09]], v100, fine, tool0;
64.       MoveL [[x1,y1,z1],[0,0,1,0],[-1,-1,-1,0],[9E+09,9E+09,9E+09,9E+09,9E+09,9E+09]], v100, fine, tool0;
65.       r1:=r1-b;
66.   ELSEIF r1>=Rmin THEN! (2)draw the circle
67.       MoveC                                     [[x2,y2,z1-zdown/4],[0,0,1,0],[-1,-1,-
1,0],[9E+09,9E+09,9E+09,9E+09,9E+09,9E+09]],[[x3,y3,z1-zdown/2],[0,0,1,0],[-1,-1,-
1,0],[9E+09,9E+09,9E+09,9E+09,9E+09,9E+09]], v100, z10, tool0;
68.       MoveC                                     [[x4,y4,z1-3*zdown/2],[0,0,1,0],[-1,-1,-
1,0],[9E+09,9E+09,9E+09,9E+09,9E+09,9E+09]],[[x5,y5,z1-zdown],[0,0,1,0],[-1,-1,-
1,0],[9E+09,9E+09,9E+09,9E+09,9E+09,9E+09]], v100, z10, tool0;
69.
70.       z1:=z1-zdown;
71.       r1:=r1-b;
72.
73.   ELSEIF r1<Rmin THEN! (3)leave from surface after finish
74.       MoveL [[x0,y0,z0],[0,0,1,0],[-1,-1,-1,0],[9E+09,9E+09,9E+09,9E+09,9E+09,9E+09]], v1000, fine,
tool0;
75.   ENDIF
76.
77.       ENDPROC
ENDMODULE

```